MSc thesis in Geomatics for the Built Environment

A probabilistic analysis of results of co-registration of **aerial** and **mobile** laser-scanned point clouds

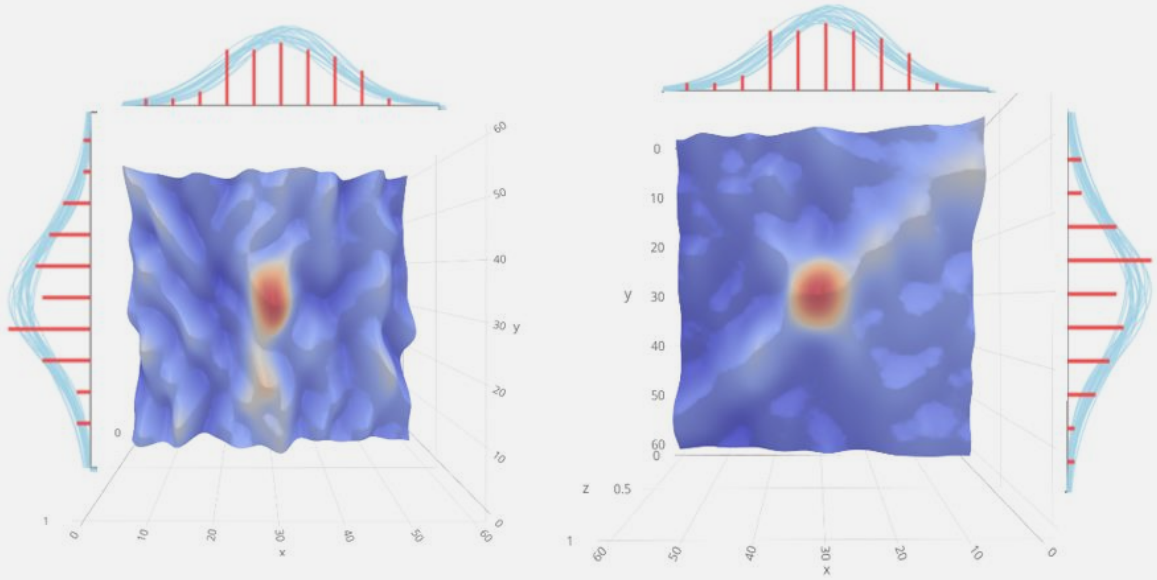

Anastasia Anastasiadou

2019

TU Delft

cyclomedia

A PROBABILISTIC ANALYSIS OF RESULTS OF CO-REGISTRATION OF AERIAL AND MOBILE LASER-SCANNED POINT CLOUDS

A thesis submitted to the Delft University of Technology in partial fulfillment of the requirements for the degree of

Master of Science in Geomatics for the Built Environment

by

Anastasia Anastasiadou

July 2019

The work in this thesis was made in collaboration between:

Section GIS Technology
Faculty of Architecture & the Built Environment
Delft University of Technology

CycloMedia Technology BV

Supervisors from TU Delft:	Prof.dr.ir. Peter J.M. van Oosterom
	ir. Edward Verbree
Supervisor from Cyclomedia:	ir. Peter Joosten
Co-reader:	Dr.ir. Freek J. van Leijen

ABSTRACT

Over the last decades, laser scanners are becoming more and more established for the acquisition of geoinformation. Depending on the sensor platform where the laser scanners are mounted, there are Mobile Laser Scanning (MLS), Airborne Laser Scanning (ALS) and Terrestrial Laser Scanning (TLS) techniques for both indoor and outdoor environments. The high-quality 3D point clouds produced from laser scanners is an important source of 3D spatial information and it is increasingly used in a wide field of applications from engineering to medical modeling, gaming and agriculture.

Although laser scanners provide dense and accurate point clouds, a scene coverage and the creation of a complete 3D representation requires multiple scans of the same area. The procedure integrating multiple scans does not always result to a perfect match. Errors that exist in the datasets or errors in the transformation of datasets create difficulties during the matching procedure. Matching data-sets with the best alignment is a topic that has been researched in many fields and a variety of methods have been analyzed for registering point clouds. A co-registration can be compared to a mathematical model and hence it is important to present not only the functional model and the set of functional relationships between the variables but also the stochastic model that describes the variability among the values and gives insights about the level of satisfying predefined demands. As a result, it becomes necessary to establish an evaluation of the output of a procedure and each result to be accompanied by its quality description.

The aim of this graduation thesis is about presenting the stochastic model of a co-registration with a quality description of the result of co-registration between point clouds. The approach will be applicable to results acquired from an image-based registration and the goal is to implement a method in order to quantify the quality of the co-registered result of two different point clouds. A probabilistic analysis of the results of an image-based method results to a quantification of the quality of the output. Response images acquired from an image-based co-registration are tested and the quality indicators of precision and reliability are determined. Moreover, the shift parameter is also defined, fact that enhances the applicability of this research to co-registrations referring to big areas where multiple local registrations have to be combined in a globally consistent manner and each local result contributes to the global registration according to its quality indicators. Particularly, response images that have clearly defined peak areas and pass the tested criteria, are considered more reliable and contribute to the global registration with a greater weight. On the contrary, blurry response images, fail to satisfy the tests, are considered less reliable results and contribute with a smaller weight.

The analysis of the images performed by testing the distribution of pixel values in both directions of the images. The implemented approach provides information about the precision and reliability of the images that have normally distributed values. Furthermore, by fitting a Gaussian line to the discrete pixel values, a sub-pixel accuracy of the result is achieved as values are generated in between the discrete pixels.

The developed method quantifies the quality of an image-based registration but further improvements and investigation of the recommendations can also attach additional value.

ACKNOWLEDGEMENTS

> If you want to go fast, go alone. If you want to go far, go together.
>
> *African Proverb*

This beautiful trip at TU Delft ended up and I can admit that it was full of unforgettable moments. Personally, I would like to thank all the people who helped me but also supported me during this trip.

Firstly, I want to express my gratitude to my supervisors from TU Delft, Peter van Oosterom and Edward Verbree for their guidance and fruitful discussions during this 8-month period. I would also like to thank Freek van Leijen who involved in this master thesis and gave me valuable comments as a co-reader.

Furthermore, many thanks to Peter Joosten from Cyclomedia company who was always there to help me, guide me, support me and answer all my questions. His responses were always immediate even during weekends and holidays !

I could not forget to thank my parents, my brother and my grandma as without their support and encouragement I could not be here and fulfill my dreams.

Last, but not least, I need to thank my new friends, here in Delft, who helped me, supported me, boosted me during my years at TU Delft. Tom, Angeliki, Elisavet, Yorgos, Ioanna thank you all !!

CONTENTS

LIST OF FIGURES

LIST OF TABLES

ACRONYMS

TLS Terrestrial Laser Scanning

ALS Airborne Laser Scanning

MLS Mobile Laser Scanning

GNSS Global Navigation Satellite System

IMU Inertial Measurement Unit

LiDAR Light Detection And Ranging sensors

UAS Unmanned Aircraft Systems

ICP Iterative Closest Point

ANOVA Analysis of Variance

UAS Unmanned Aircraft Systems

1 INTRODUCTION

1.1 PROBLEM STATEMENT AND MOTIVATION

Nowadays, there is a high demand for 3D information in different fields and applications. As a result, active sensors as laser scanners have been established in the field of Geomatics because of their ease of use in the field and due to the vast amount of 3D data that can produce rapidly. Light Detection and Ranging sensors (LiDAR) are the most successful techniques for data acquisition (Lemmens [2011]). Dense and accurate 3D point clouds can be produced by LiDAR and they are a significant source of 3D spatial information.

The general principle of laser scanning is the procedure that using laser beams, distances and angles are calculated, and surfaces and objects are sampled. A scanner emits a pulse to a surface, and it records the time needed for the reflection of the pulse back to the scanner. As the light travels with a known constant speed, the distance between the sensor and the surface can be calculated. Repeating this process for multiple times, a 3D representation of the scanned environment occurs as thousands of 3D points are recorded resulting to a 3D point cloud.

Depending on the sensor platform where the laser scanners are mounted, there are Mobile Laser Scanning (MLS), Aerial Laser Scanning (ALS) and TLS techniques for both indoor and outdoor environments. An MLS is a technology that combines LiDAR sensors with a GNSS receiver and an IMU mounted on mobile platforms as cars, vans or vessels. GNSS receivers are useful as they provide information about the position of the sensor and the IMU determines precisely the orientation of the sensor. The combination of information from GNSS receivers and IMU mounted on recording vehicles determine the vehicle's position and orientation. Therefore, with the knowledge of the position and orientation of the vehicle, the 3D coordinates of the scanned points can be computed as a function of distance and angle. ALS techniques consist of the same technology but they are mounted on helicopters, airplanes or Unmanned Aircraft Systems (UAS). Lastly, TLS techniques are the static scanners mounted on static tripods over the ground.

Environments with different characteristics require different techniques for scanning. Usually for works that require 3D spatial information for small areas or indoor environments, static platforms are used. On the contrary, for works that require scanning of larger areas as whole neighbors, cities or inaccessible places, mobile or aerial platforms are necessary. Most of the times, MLS techniques are preferred due to the spatial resolution of data acquired (Bae and Lichti [2008]) and the required time for the measurements which is significantly less compared to the traditional static survey methods.

Various devices allow acquiring appropriate representations of surfaces or objects using 3D point clouds. Although line-of-sight instruments can provide dense and accurate point clouds, a scene coverage or objects with complex geometries require multiple scans of the same area (Weinmann and Jutzi [2015]) as laser scanners have a limited field of view (Bae and Lichti [2008]). Therefore, the creation of a complete 3D representation requires a combination of all the different laser scanned elements from different angles and a proper calculation of transformation parameters for achieving the best merged result.

1.2 INTEGRATION OF DATASETS

The procedure of integration does not always result to a perfect match. Errors that exist in the datasets or errors in the transformation of datasets create difficulties during the matching procedure. A receiver, in order to estimate its position coordinates and a clock bias needs to observe at least four satellites (Ogaja [2011]). In cases with poor or absent of GNSS signal, this estimation is impossible due to occlusions and moving objects in the datasets. As a result, faulty measurements with translational (x,y,z), rotational (yaw) and scale errors occur. Especially in urban areas, reflections of objects can lead to erroneous measurements (Shetty [2017]). Big obstacles and high buildings can restrict the visibility of the GNSS signals and make the positioning calculation less accurate creating also less accurate measurements (Figure 1.1).

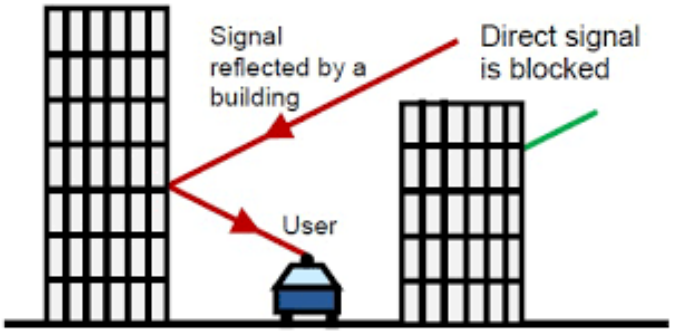

Figure 1.1: Big building restrict the visibility of the GNSS satellites and make the calculation of the positioning impossible (Zhu et al. [2018]).

Such inaccuracies can be partly addressed with the use of GNSS receivers integrated with IMU and odometers that enable to geo-reference the data collected by the sensors and obtain accurate positions (Lemmens [2011]). Besides the positioning errors due to the limited GNSS signal, there are also orientation errors around the z axis, called yaw angle errors. Yaw errors usually occur when the recording vehicle takes successively the same direction in turns (Christodoulou [2018]). For this work, only translational errors are taken into consideration and yaw and scale distortions are considered negligible as the datasets are considered to be free of yaw and scale errors.

Matching data-sets with the best alignment is a topic that has been researched in many fields as photogrammetry, computer vision, robotics. It is also essential for

the agriculture as relevant information is obtained for the ground cover or the development of the plant. Co-registration can be determined by the process of matching different 3D point clouds. A variety of methods have been analyzed for registering point clouds as a reliable reconstruction is an important prerequisite for various tasks as city modeling, scene interpretation or urban accessibility analysis (Weinmann and Jutzi [2015]).

The co-registration can be achieved either by using feature-based techniques that include geometric primitives, shape descriptors and patterns or image-based techniques that use photogrammetric principles with the ultimate target to transform all different partially overlapping scans into a common reference system.

A co-registration can be compared to a mathematical model and hence it is important to present not only the functional model but also the stochastic model. The functional model includes the sets of functional relations that connect the variables in order to reach the perfect result. However, since the measurements are never perfect, the variability among the values must be taken into consideration. This is achieved by the stochastic model in which the measurement uncertainty is described by stochastic variables. The stochastic model gives also an insight about the level of satisfying predefined demands. As a result, it becomes necessary to be established an evaluation of the output of a procedure and each result to be accompanied by its quality description.

1.3 ULTIMATE TARGET OF THIS RESEARCH

The aim of this graduation thesis is about presenting the stochastic model of a co-registration with a quality description of the result of co-registration of point clouds. The approach will be applicable to results acquired from image-based registration either produced via laser scanning platforms or extracted from aerial photos using suitable techniques as for instance, a dense matching technique that generates point clouds. A probabilistic analysis of a co-registration of different point clouds will be presented, in terms of two quality indicators, reliability and precision.

The goal is to implement a method in order to quantify the quality of the co-registered result of two different point clouds, either acquired from the same source or from different sources. Although the outcome can have a wide application, for avoidance of multiple complexities the focus will be the analysis of an image-based co-registration of point clouds from aerial and mobile laser scanned point clouds acquired from LiDAR.

1.4 IMPORTANCE OF EVALUATING A RESULT

But why it is important to investigate the quality of a registration? As the scientific and commercial field is getting more and more demanding and in combination with the increasing complexity and automation of processes, a way to quantify

the quality of a product or a service will lead to more reliable and trustworthy results.

It is surprising that although the functional part of a matching algorithm is vastly addressed by various approaches, the stochastic properties have received little attention. The reason can be the complexity of the topic or the deficient knowledge for the importance of understanding the actual result and therefore its degree of quality. A result should be combined with its quality description, so that a conclusion can be made about satisfying certain specifications or not.

Moreover, in cases where the results of a co-registration can be used for a future, non-local but more generic global registration, it is necessary to estimate its quality as it is the only way to assign to each result an equivalent weight. Most of the projects only deal with the procedure of the matching of point clouds, the duration of the algorithms for the implementation and give little attention to the quality of the final result. The importance of the real meaning of estimating the quality is still unremarked and this stimulated the initial motive for a graduation thesis with such a topic.

1.5 RESEARCH OBJECTIVES AND RESEARCH QUESTION

The goal of this approach is to go a step further from the before-mentioned approaches by taking the results of a co-registration of two point clouds and estimate the quality of the result of the matching (Figure 1.2). Namely, it is believed that the estimation of the quality of a result is as significant and necessary as the result itself. As little attention had been given to the quality indicator in the past, this will be a research about quantifying the quality of a local registration and create a significantly valuable base for a global registration.

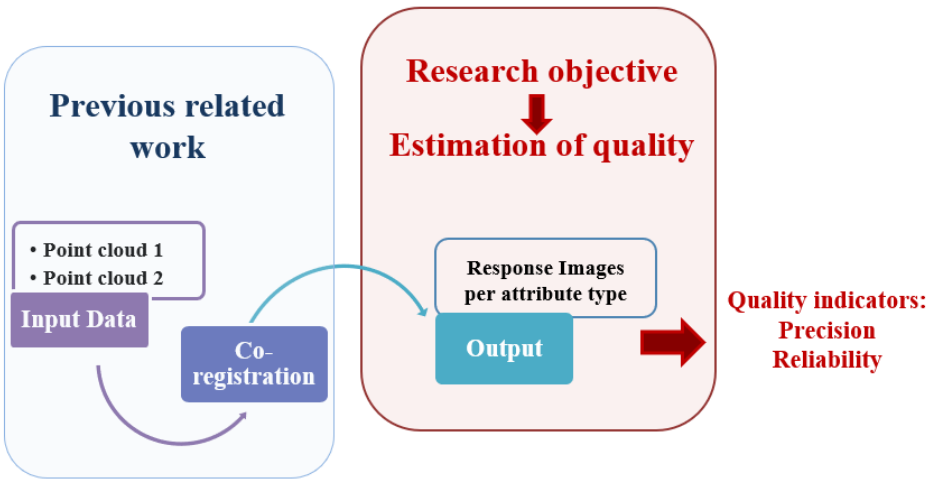

Figure 1.2: Previous related work on registration and the approach of this graduation thesis topic

Therefore, the main research question is framed as:

To what extent is it possible to estimate the probabilistic aspects of the result of a co-registration between aerial and mobile laser scanned point clouds ?

Some sub-questions that are relevant and will be answered during the analysis are:

- What are the requirements for a registration?
- Is this technique of co-registration suitable for every case?
- How can the probabilistic analysis be performed?
- Could a probabilistic analysis reveal that the requirements are not met?

1.6 THESIS OUTLINE

The next chapters are structured as follows:

- The second chapter presents a general background with useful theoretical information, terms, techniques and methods that are used in this thesis. Also statistical terms and their relevance with the estimation of quality are present.
- The third chapter includes an analysis of previous related work. Various different methods and approaches are found in the literature about the co-registration of 3D point clouds using either 3D or 2D based methods.
- The fourth chapter consists of a description of the datasets used, the software and hardware that is necessary in order to carry through with this research.
- The fifth chapter provides an analysis of the implemented methodology and also results that are obtained. An analysis of response images from a co-registration between point clouds is performed, with the aim of estimating their quality. The analysis implemented using the distribution of images' values. The precision and reliability of each response image is determined, important parameters that characterize the quality.
- The sixth chapter contains how the research questions are answered and some conclusions. Also, future recommendations are drawn about the next steps of this research and how it can be extended.
- Lastly, a reflection on the value of this graduation thesis work in the scientific field is given.

2 THEORETICAL BACKGROUND

This chapter gives the general information about theoretical terms, techniques and methods that are used in the current research. Definitions about the terms of registration, characteristics of a local and a global registration, quality indicators that characterize their results are given. Moreover, statistical terms are also discussed as they constitute a significant part of this work.

2.1 CO-REGISTRATION

Data registration is the transformation of the coordinates acquired from different scans from different perspective points depicting the same area, into a common coordinate system (Gümüş et al. [2017]). Registration or co-registration refers to the process of matching different point clouds that have common characteristics. According to Chen and Medioni [1992], two views of a surface are registered only if they "coincide" after placing the first view at a proper position and orientation respective to the second one.

A co-registration can be divided into two main categories: the local and the global registration. Local registration is a first pairwise alignment that leads to a first local result while the global registration is the next step, that integrates all these individual local alignments so that they all match together resulting to the perfect global alignment (Figure 2.1).

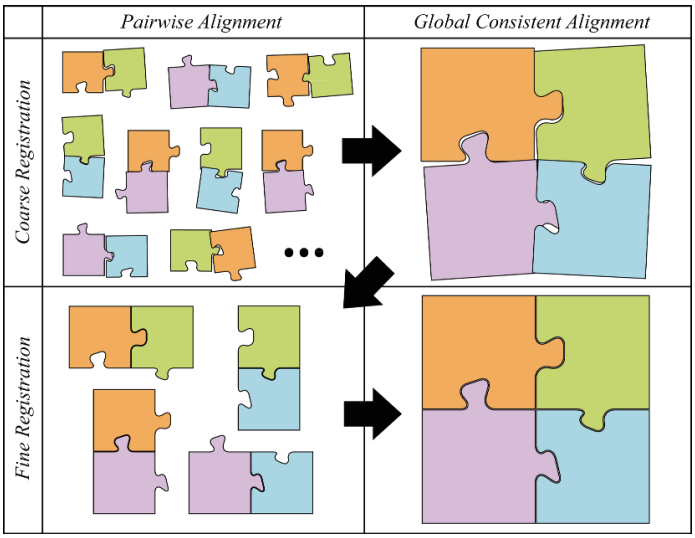

Figure 2.1: Globally consistent registration of terrestrial laser scans Theiler [2015]

The accuracy of the final result of a registration is related to two kinds of errors: the acquisition and the registration errors (Bergevin et al. [1996]) as except from the data quality that depends on the equipment and the surroundings, the distribution of the residuals errors of the separate pairwise alignments also contribute to the final accuracy (Benjemaa and Schmitt [1999]). A global registration can be considered as an optimization problem where the optimal solution is the one that minimizes a predefined cost function (Kamgar-Parsi et al. [1989]). Global alignment has as aim to properly distribute the eventuated errors in the previous step. Finally, a global perspective can also enforce consistency among the local alignments as improving the quality of a global matching, the errors in local scale are also reduced (Kamgar-Parsi et al. [1989]).

There are various ways to co-register point clouds, either 3D-based, where 3D control features are used for the registration or 2D-based methods where images are extracted from point clouds and compared. In both cases, a template is iteratively compared with the sample in order to determine optimal set of correspondences but also the transformation parameters between the source and target.

2.2 IMAGE-BASED REGISTRATION METHOD

3-D point cloud can be matched by using a 3-D data registration using control features as control points, control lines or control surfaces (Teo and Huang [2014]) but also by extracting multiple planes or images from them, resulting to 2D image registration. There are algorithms that use low-level features as edges and corners, algorithms that use high-level features as identified objects or relations between features or algorithms that use image pixel values (Reddy and Chatterji [1996]).

Image registration comprises the procedure about matching images that contain common visual information but also differences due to different views or different type of instruments (Gaidhane et al. [2014]). It can be considered as a geometric alignment of a set of images with the goal of establish a geometric correspondence between them and afterwards they can be analyzed, transformed, compared into a common reference system (Wolberg and Zokai [2000]).

In cases of 3D point clouds, extracted planes from the point clouds are treated as images in order to perform a template matching. More specifically from each point cloud, different planes can be acquired depending on the selected projections. The most typical examples of extracted planes are by splitting the 3D point cloud into 2D projections in pairs of X,Y and Z axis (Figure 2.2) and therefore the planes or projections can be treated as images. However, there are cases of researchers who used other approaches and the directions of the images are created from important planes present in the scene. A significant indicator in that latter case is the reduction of planes into lines in each view directions in order to create meaningful projections.

Image-based registration has practical importance in many fields as remote sensing, medical imaging, computer vision as it is often necessary to integrate images

acquired from different sensors, at different times and under different conditions. Template matching is the most typical method used for image integration.

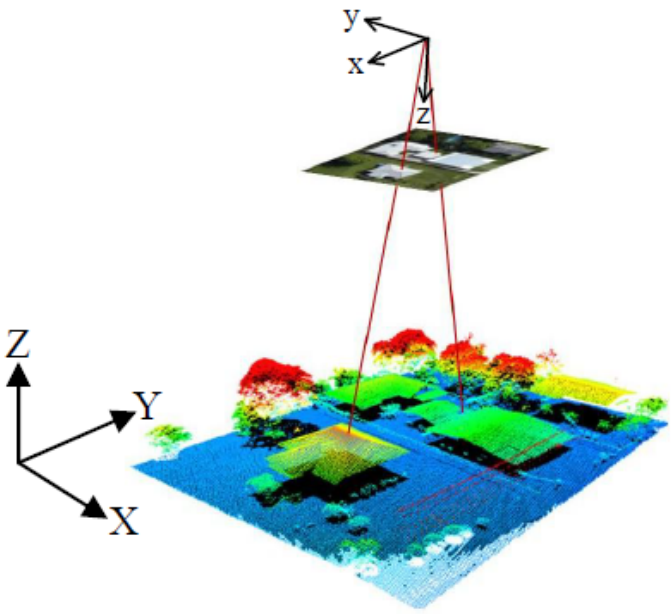

Figure 2.2: From a 3D point cloud, 2D planes are extracted. (Parmehr et al. [2012])

2.3 TEMPLATE MATCHING

Template matching is a technique for identifying areas that are similar to a specific pattern. It has a wide variety of applications in different fields of research and especially in image processing. It does not require pre-processing of the data as cross-correlation techniques can struggle with multiple limitations (Guizilini and Ramos [2018]). Although template matching is quite popular and three dimensions are more representative of the real-world environment than single 2D parts, only a few recent attempts have been made to jump from two dimensional to three dimensional datasets.

VanCourt et al. [2005] and Jurie and Dhome [2001] present some typical examples using 3D template matching but the implementation was performed using 3D objects with known attitude. More complex objects or environments with multiple objects, require multiple rotations and interaction matrices. Additionally, 3D calculations except from three-axes rotations, bring various computational complexities, high non-linear projective transformation parameters, time-consuming procedures and require 3D memory structures, as instead of 2D grid cells with pixel units, 3D grid cells with voxel units and transformation parameters to be combined in all three dimensions are necessary.

2.4 TEMPLATE MATCHING FOR IMAGE-BASED REGISTRATION

Template matching can be also used for image-based registration. The images are extracted planes from the point clouds in all possible pairs of projections and the matching is about determining the presence and location of a template image within a reference image (Ding et al. [2001]). Generally, it is used for comparing portion of images (a template image), against another image (an input image) resulting to an output image. After iterating shifts of the template image to all possible positions in an input image, numerical indexes are computed indicating the degree of the matching in each position (Figure 2.3). The purpose of a template matching is the decision about how similar are the input images. Once the templates are found, their centers are kept as control points to determine the registration parameters. The whole process consists of a cross-correlation technique between the template and the reference image so to compute a measure of similarity and therefore determine the respective displacement (Zhang et al. [2009]).

There are also examples of works where template matching is performed using images, created from point clouds acquired from different sources but referring to the same area (Christodoulou [2018] and Someren [2016]). Iterating shifts of images of the first point cloud over the respective images from the second result to the response images that contain the values of the scores of the matching.

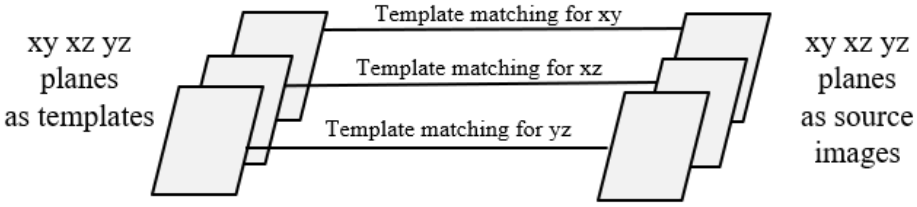

Figure 2.3: Basic schema of template matching using planes

The actual result of the template matching procedure in the co-registration of images is response images consisting of values, the similarity values. Similarity values indicate the degree of the matching between the input images. The higher the values, the better the matching and the brighter the respective parts of the response image. On the contrary, smaller values are assigned to less good matching and are the darker parts of the response image.

There are various ways to combine the input image when performing template matching and lots of different attributes of an image that can be used. Examples of attributes can be the point density of an image, the intensity values of an image, the gradient of the intensity of an image, the depth of an image, the height gradient of an image, the color gradient, the gradient of the depth etc. For instance, the following images show density and color images and their respective responses (Figures 2.4 and 2.5).

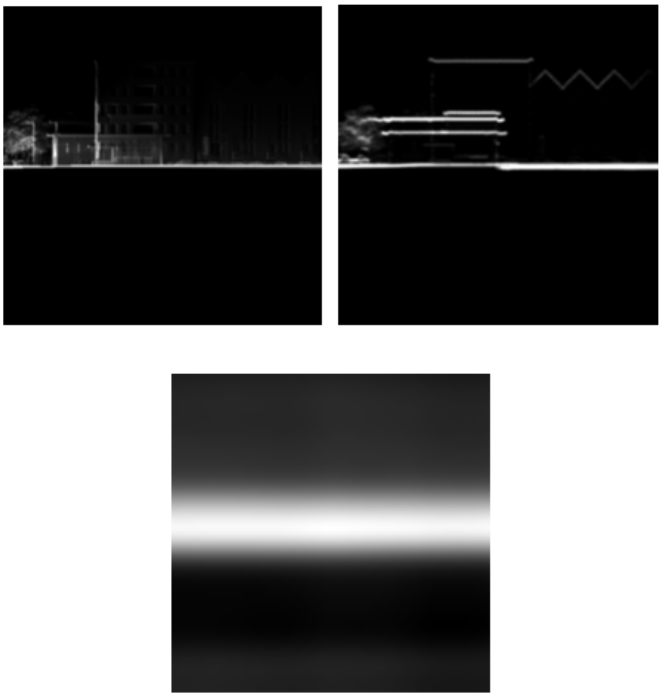

Figure 2.4: At the top, two input images are compared using a template matching. At the bottom the result from the template matching, a response image. All images are created using the image attribute of the density.

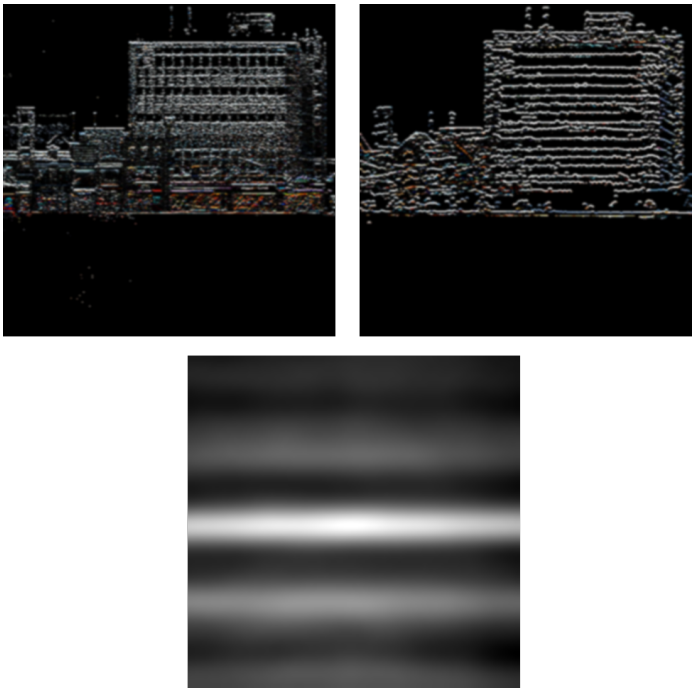

Figure 2.5: At the top, two input images are compared using a template matching. At the bottom the result from the template matching, a response image. All images are created using the image attribute of the color.

A brief representation of the basic steps of template matching is presented so to become clear how the response image is created. For the ease of the representation two input images are transformed to have transparent background and different colors. The template matching starts from the initial position where the centers of

two input images coincide as it is visible in Figure 2.6. The next steps of the template matching are performed by shifting the first image by 30 positions equals to the pixel size to the left, 30 positions to the right, 30 positions up and 30 positions down in the second image, as it is shown in Figure 2.7. After the iterating shifts, the matching scores are calculated and the response image is extracted.

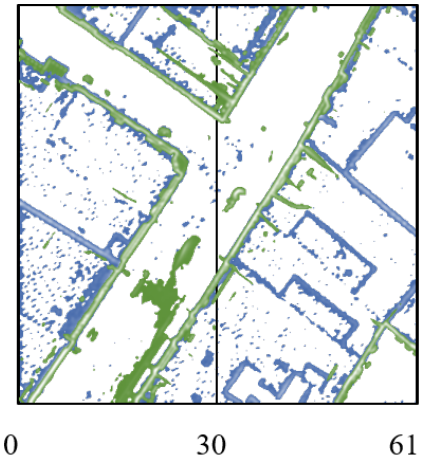

Figure 2.6: Initial position where the centers of the input images coincide.

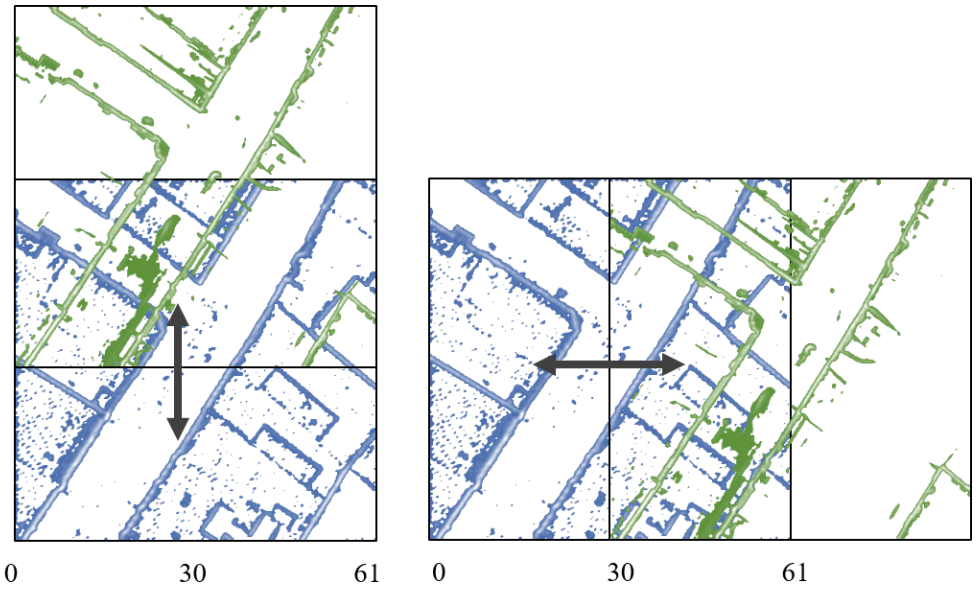

Figure 2.7: Iterating shifts of the first image over the second image in all possible directions.

In Figure 2.8 the response image and the matching scores can be shown using a response image in 2D and a part of it using a heatmap containing also the arithmetical matching scores. The darker are the values, the lower are the numbers in the corresponding pixel locations and they belong to the blue regions in the annotated heatmap. On the contrary, higher values are the brighter parts of the response image and they belong to the respective orange and red parts of the annotated heatmap.

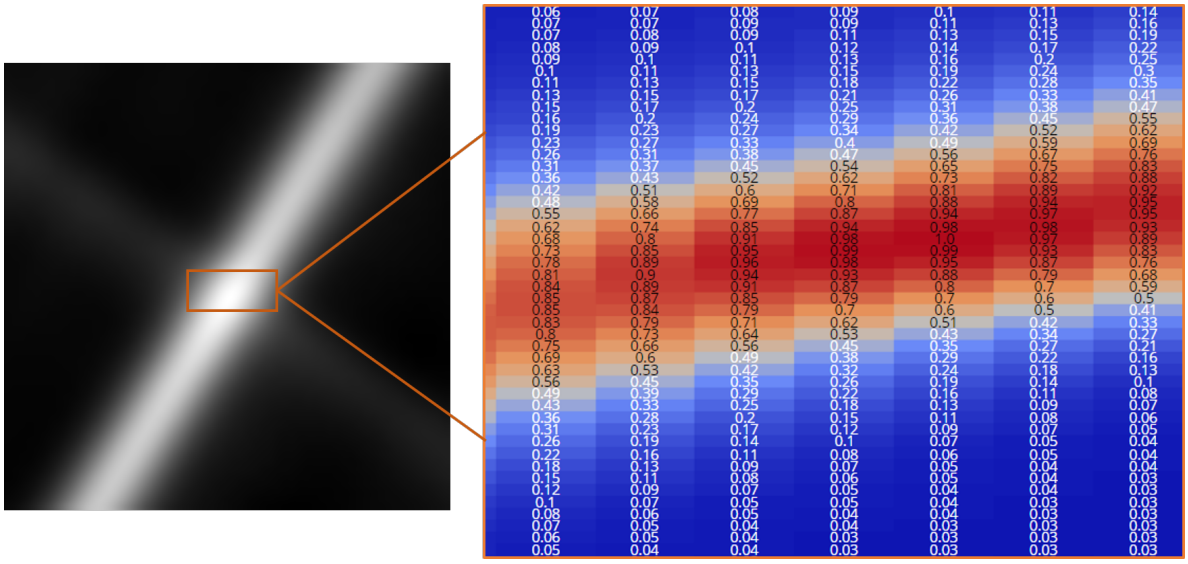

Figure 2.8: The response image, result of the template matching on the left & a smaller part of the response image depicting the similarity scores on the right

It can be easily distinguishable that the response image depends on the input images. In cases where two images slightly differ, the response image has discrete parts that are brighter. Similarities that follow linear behavior in input images result to a response image with linear brighter parts as it is shown in Figure 2.4. On the contrary, input images that do not have specific common parts, either because the similar parts are not at the same location or are not visible at both images, result to more blurry and fuzzy response images that do not give a clear impression of the existing situation as in Figure 2.5. A detailed analysis of the response images including also statistical terms will be presented in a next session.

2.5 QUALITY OF CO-REGISTRATION

The quality of a co-registration between an MLS and an ALS point cloud is characterized by two different quantities. The quality partially depends on the actual output after the acquisition part, conclusion that can be derived by evaluating the proper use of the equipment and proper scanning and partially it depends on the way of integrating datasets and accepting or rejecting the calculated parameters. Consequently, quality is a term that can be addressed by estimating the quality of each individual dataset and afterwards the quality of the integrated result.

Following this chain, the analysis of the results is a key element for evaluating the quality of a process. Information about the degree of correctness and the quality of an alignment is crucial and especially in applications dealing with the real world (Bogoslavskyi and Stachniss [2017]). This work aims to present a quantitative approach for the evaluation of the quality of the co-registration procedure based on a probabilistic analysis of its results, the response images obtained from an image-based registration.

Generally, every functional model, for instance a co-registration of point clouds must be accompanied with a stochastic model. The functional model includes the

functional relationships between the variables while the stochastic model is about computing estimations of quality measures about the acquired results from the functional model (Teunissen [1998]). A quality model is a conceptual framework in which the term of quality is gradually analyzed. Using a quality model, the quality of product or process can be compared and described. Generally, the main parts of a quality model are characteristics and parameters. Each characteristic is described by some parameters. The parameters substantiate the characteristics and can be quantified with specific values as for example the standard deviation σ (Kutterer et al. [2016]).

2.6 OPTIMAL SOLUTIONS

It is difficult to assess whether or not a solution is optimal due to distortions in the datasets or errors during incorrect operations through the editing processes, such as the template matching and the determination of the transformation parameters. Moreover, optimal solutions are not always satisfying enough or valuable for use. For example in cases that the template matching is performed in point clouds with small densities and limited information, the result can be the optimal from the possible outcomes but still it can be not representative of the region and hence not useful. So, another significant aspect that must comprise a part of such work is the quality of the given solution and ways of its quantification, as quality control has gained importance in survey work due to the developments in the instruments.

Generally, in geodesy, an optimal solution is usually obtained by using the least squares adjustment. It is based on the criterion that the sum of squares of the observational residuals must be minimized. After performing a least squares adjustment, the best possible solution based on the available observations can been found. Having determined a solution, it is important for the researcher to be able to estimate the quality of it via indication.

Quality in geodetic projects is the degree of satisfying the predefined demands of a customer (Teunissen et al. [2005]). Probabilistic models are often used in engineering in order to express the relations between the data, the parameters and the uncertainties. It is important to formulate such probabilistic models, to combine data but also to estimate and judge the quality of the results computed (Teunissen et al. [2005]). As Teunissen et al. [2005] also mentions, quality measures needs to be provided for the results of every research, so to make them useful and practically relevant, as only displaying values, is 'just values without a value'.

At the same vein, in case of a co-registration between point clouds there are only a few tools that can diagnose the quality of the matching except from the visual inspection of the alignment (Pulli [1999]). In this project the focus will be on testing how well the alignment has been performed by using as quality measures for the analysis the precision and reliability.

2.7 PRECISION OF CO-REGISTRATION

The precision of a geodetic network can be defined as the influence of the stochastic variabilities of the network observations on the coordinates (Sweco [2019]). Teunissen et al. [2005] refers to the spread or variability in the estimated result in an iterative process under similar circumstances. Geodetic observables are stochastic variables and can be described only by stochastic models. Consequently, the quality is described by stochastic variables. It cannot be expressed by a single value due to deviation in errors and it is best described by a probability distribution which gives an insight about the relation between the standard deviation and the probabilities of the errors. At the same vein, the outcome of the co-registration is also explained by a stochastic model and hence, deviation of the values around a specific value characterizes the precision of the examined sample.

Therefore, tests for the distribution of the samples will give indications about the precision and afterwards the quality of the outcome. Normal distribution is often assumed. So, it is becoming important for the research to test the normality of a distribution and verify it except from simple suppositions. Examples of normal distributions with different mean values and variances are presented below (Figure 2.9). As standard deviation characterizes the samples, the greater the deviation between the values the less precise the data.

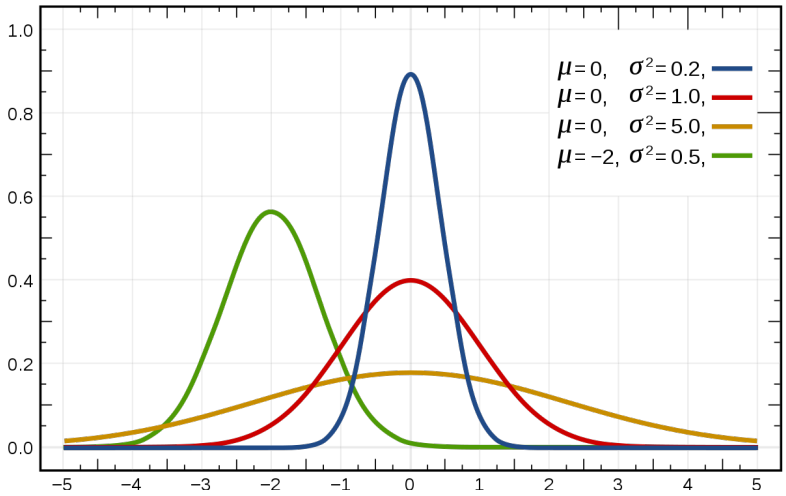

Figure 2.9: A representation of normal distributions with different standard deviations and mean values

However, precision only measures the amount of the variability in the tested sample around a mean value, measurement that is sufficient only when the estimators are unbiased. In case of a co-registration, the unbiasedness of an estimator is not necessary known as it depends on the selected method and variables (Teunissen [1998]). So, another measure must also be provided, and this can be the reliability that will further analyzed in a next session.

2.8 TESTING THE DISTRIBUTION

The normal distribution is the most widely known and used of all distributions. As the normal distribution approximates well various phenomena, it has developed into a standard reference for probability problems. Gauss also showed that normal distribution is the only one for which the maximum likelihood estimates equals the arithmetic mean, which is the correct solution for the parameter estimation (Ober [2004]).

Most of traditional quality control methods are based on the assumption that the measurements follow a normal distribution. Hence, normal distribution is going to be examined, as it is the most dominant distribution in this field. Fact that can be explained as in normal distributions precision can give significant indications for the quality of the data and it can be linked to probability analysis. As a result, when it is applicable, it is important to prove the existence of a specific distribution with a statistical test and not only assume it.

The distribution of pixel values of response images are tested with statistical tests. A statistical test is a hypothesis proposed for a statistical relationship between two datasets which is compared to an idealized null hypothesis. The comparison is characterized significant only when the relation between the datasets is a realization of the null hypothesis according to a threshold probability (the significance level). The critical values of a statistical test are the boundaries of the hypothesis acceptance and they are determined by the choice of a level of significance α.

In this specific work, the results from a template matching are analyzed and tested whether or not they are normally distributed in order to draw conclusions about their quality and consequently the degree of success of the template matching.

2.9 TESTS FOR NORMAL DISTRIBUTION

There are various tests existing in the literature for testing the normal distribution of a given dataset. Kolmogorov-Smirnov test (KS-test) is a test that can be used to compare a sample with a reference probability distribution or to compare two different samples. KS-test quantifies the difference between the empirical distribution of the samples. From the null hypothesis, the null distribution is calculated. In the case of testing for the normality of the distribution, the samples or the observations or the selected variables are standardized and compared with a standard normal distribution (MIT Open Courseware [2019] and Wikipedia [2019]). A statistic value and a probability value are the outputs of the test. After selecting an alpha value (α), the comparison between alpha and the extracted statistic value will give a response about satisfying or not the null hypothesis and consequently having or not a normal or Gaussian distribution.

Another test for normal distribution is the Shapiro-Wilko test which estimates the variance of the sample in two ways: firstly, the variance of the datasets is calculated using a regression line and secondly the variance is calculated as an estimator of the

population variance. In case of normal distributions, both values should be similar and close to 1.

The tests will be implemented using input values from the response images. The knowledge on the distribution of a dataset is also crucial for another reason. Based on the distribution, conclusions can be derived about the most suitable way to cluster the dataset. An analysis of the distribution shape can aid in a construction of a clustering algorithm with a proper cluster size and centroid (Burghouts et al. [2008]).

2.10 RELIABILITY OF CO-REGISTRATION

Modern total stations and GNSS receivers are capable of producing a great amount of survey data, as well as demanding efficient tools for assessing their sufficiency and accuracy (Sweco [2019]). The difference from the older measurement methods, with only single point measurements, is that the current ways for acquisition of data lead to huge datasets that require other ways to be tested and analyzed.

In the specific case of this work, point clouds are acquired from MLS and ALS techniques. Each MLS recording device is equipped with a GNSS receiver and an IMU so to determine vehicle's position and orientation. As a result, a LiDAR mounted on a mobile platform (Figure 2.10) records distances and angles between the device and the scanned environment and combined to the known position and orientation information, the coordinates of the scanned environment can be calculated as a function of the distance. ALS point clouds are LiDAR data acquired from a Leica CityMapper which is a hybrid airborne sensor that combines oblique and nadir imaging with LiDAR data into one sensor (Leica Geosystems [2019]).

Figure 2.10: A LiDAR sensor, a GNSS receiver and an IMU mounted on a mobile platform of the company Cyclomedia Technology B.V.

The reliability of a system has been analyzed for various fields, for example by filtering bad co-registration results with ratio between first and second peak in the response image, threshold and overlap. According to Teunissen et al. [2005], is approached by referring to how well can errors, anomalies and misspecifications of a model can be traced and how sensitive are the final results to errors, anomalies and misspecifications that remain undetected. Moreover, it is described by the ability of the observation system to test for modeling errors (Teunissen et al. [2005]). The reliability of a network can be also described in terms of the sensitivity to the detection of outliers (Sweco [2019]).

More specifically, the term reliability can be split into internal and external reliability. Internal reliability is the size of the smallest possible observation error (Christodoulou [2018]) and it can be expressed by the Minimal Detectable Bias (MDB). It determines in which degree an error of an estimation is detected. External reliability is used as a measure to determine the influence of a possible and undetected error in the observations on the adjusted results (Teunissen et al. [2005]). Thus, results that include undetected errors have poor external reliability.

The general theory about reliability and how it is calculated is obtained from (Teunissen et al. [2005]) and although the theory is about geodetic observations and surveying methods , the basic elements are adjusted in order to be used for estimating the reliability for the results of a co-registration as they also contain spatial information.

2.11 GLOBAL REGISTRATION

A global registration can be considered a step further from local registrations. For instance, in registrations referring to a whole city or a whole country, multiple point clouds have to be aligned in a globally consistent manner. The procedure is achieved by dividing the whole area into multiple smaller pair-wise registrations (Figure 2.11). These smaller pair-wise registrations are necessary for a better handling of huge datasets. The optimal way of combining all the individual local registrations is by introducing a criterion for good, less good and poor results. This criterion incorporates the term of quality and hence, results with good quality values participate with higher weights in a global registration.

2.11.1 Example of a global registration for the whole country of the Netherlands

Using as example a global co-registration for the country of the Netherlands, the whole area is divided into tiles with equal size. Each square is referring to a local co-registration between point clouds for a specific area. In order to move from local to global registration, each tile should contain not only the actual co-registered result of point clouds, but also parameters that indicate its quality. Quality parameters are the key element in order to create an accurate global registration by combining all the intermediate calculated parameters for the local registrations but at the same time considering also their quality result. An approach for addressing the quality is analyzed in a next section.

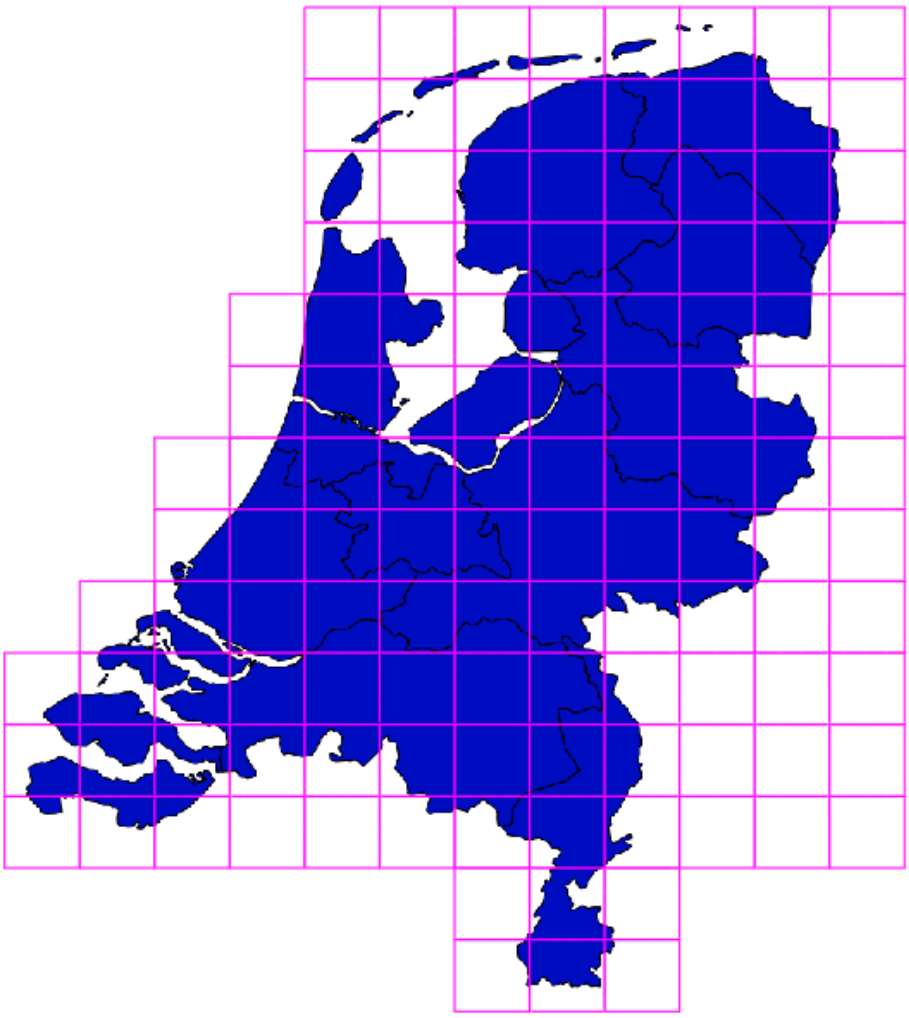

Figure 2.11: Tiles represent all the individual segmented parts

2.11.2 The evaluation of the results

Local registrations can be accompanied by parameters that describe the estimated quality and can be visualized by arrows. Arrows include information about the shift and how much the center of each tile must be moved and in which direction in order to be achieved the perfect matching. Different lengths of arrows indicate different size of the shifts and different thicknesses represent smaller or bigger values of standard deviations of measurements. Empty tiles can be used for results that do not have an acceptable matching and they are not participate in the final global registration.

The evaluation of the results and therefore the arrows that characterize each tile is performed in two consecutive steps. The first step is about calculating the parameters for the co-registrations and the tiles obtain the respective arrows. The second step is about evaluating the arrows and characterize the respective tile as reliable or not.

The criterion for classifying the resulting arrows is whether or not they follow similar behavior with their neighbors. Similar behavior can be described by how smooth and gradual is the direction and length of arrows from one tile to its consecutive

or neighboring. Results that deviate significantly are judged as less reliable. They are possibly faulty measurements as for instance, errors that occur due to positioning errors of the equipment during the acquisition of the data especially in urban environments. These examples comprise less satisfactory results for the final global registration.

Lastly, at the vice versa consideration, setting adequate weights to each separate tile based on the quality results of each individual local registration will enhance the quality of the final global registration (Figure 2.12). Moreover, considering the practicality of the procedure, a global registration can be an extra check as even if it fails to assign the proper values to the individual tile, it can still provide important information about the location of the problem (Theiler [2015]).

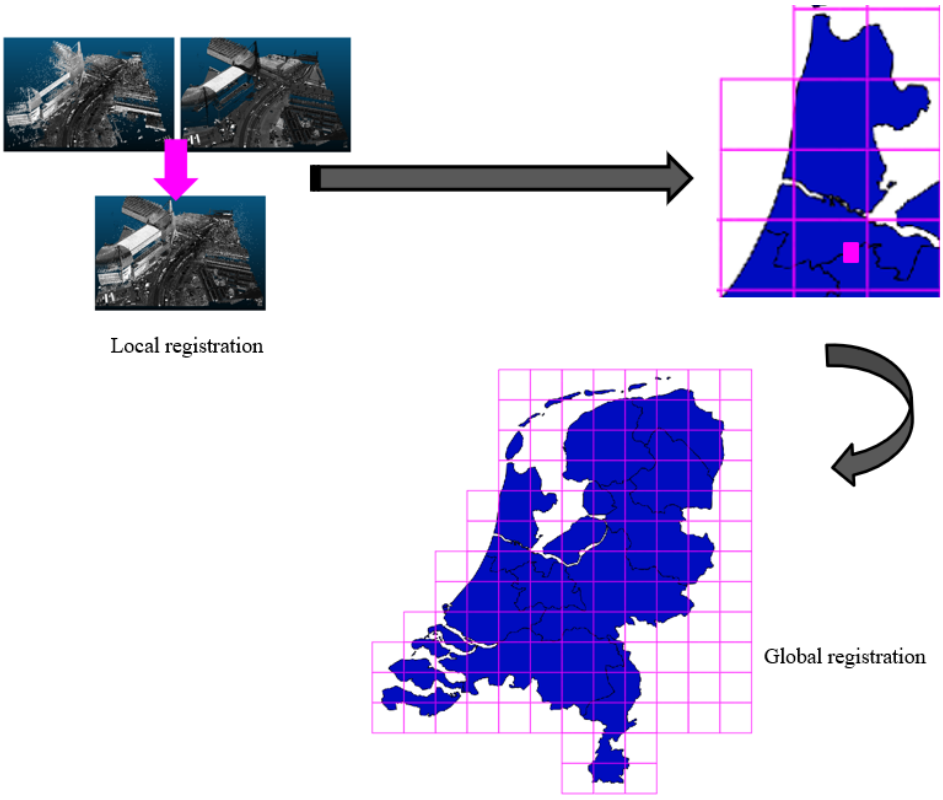

Figure 2.12: Individual results of local registrations are used for a global registration

This graduation work has as aim to set a base for quantifying and estimating the quality of the result from an image-based registration. An example with calculated shifts and results for neighboring tiles are presented in a next chapter. Further research is necessary for finding a model that simulates the behavior of the arrows in tiles, so to cluster them in respective neighbors, compare the different results and assess when a tile should be ignored or not.

2.12 CO-REGISTRATION IN RELATION TO GEODETIC NETWORKS

Baarda's concept for the assessment of quality of observations and least square adjustment is accepted in photogrammetry and geodesy (Baarda [1968]). Assuming that there is a relation between geodetic purposes and co-registration of point clouds, the same concept can be also applied as well. Error propagation in geodetic networks can be compared to weights propagation in the results of co-registration.

Comparing to the procedure of a network leveling in geodesy, where the error is divided into all the measurements using a Least Square Adjustment, in the case of a co-registration, a quality indicator characterizes each local pairwise co-registration in a way that a better quality indicator results to a bigger weight to a local registration and a big contribution to the global registration while on the contrary, results with a less good quality indicator lead to smaller weights and a smaller contribution to the global result. The confidence ellipses that depict how the error is propagated in geodesy are replaced from arrows that characterize each local registration. In that vein, as Least Squares Adjustment minimizes the errors, the weight adjustment also minimizes the errors in a different way, by minimizing the influence of erroneous local registrations to the global registration as adequate weights for each tile contribute to more accurate results.

Although there are many similarities between the results from co-registration and geodetic procedures there are also some differences. Firstly, in geodesy there is redundant information and redundancy is used for estimating the accuracy of the positions. Secondly, in a geodetic network the final deliverable is known and the potential permissible misclosure must be within some predefined limits to be acceptable. For instance, when a geodetic traverse is about to be solved, which is either closed on itself, or it is between points with known coordinates (triangles) (Figure 2.13), there are known parameters that set constrains to the final solution.

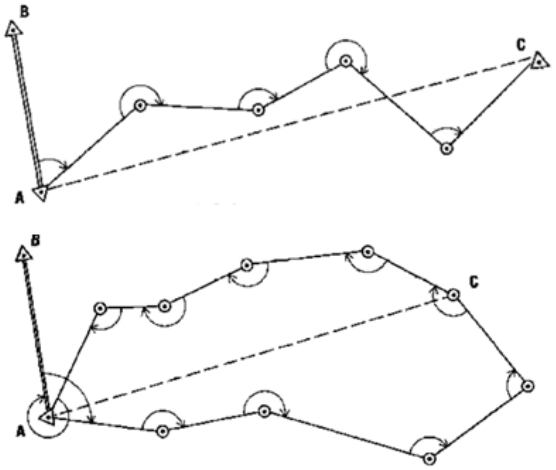

Figure 2.13: At the top an open geodetic traverse between points with known coordinates. At the bottom a closed geodetic traverse

Another example from surveying that can be compared to the procedure of a co-registration is the errors analysis in GPS measurements for setting realistic parameter uncertainties. Through the analysis, the errors are not minimized but they are classified, conclusions about their source can be provided and precision and accuracy can be improved (Williams et al. [2004]).

The next chapter presents some typical examples of related work that are based on the analyzed theories.

3 RELATED WORK

The creation of 3D models of a real world requires except from a stage of data capture, a registration stage which aligns all the different views and a last stage that merge and simplifies the previous aligned views Sharp et al. [2002]. In case of 3D point clouds, all the sequential registrations of the obtained independent point clouds are referring to a common area with a significant percentage of overlapping. Registration is a procedure to minimize the inconsistency between two different point clouds Teo and Huang [2014].

The registration of point clouds is usually conducted in two consecutive steps, a first coarse registration of sufficient quality followed by a fine registration (Wang et al. [2016]). A considerable amount of previous work has been done for registration of point clouds acquired from laser scanners with researchers from multiple fields as computer vision, artificial intelligence, photogrammetry. Various methods and different solutions have been implemented and some typical examples are analyzed in this section.

3.1 ICP ALGORITHM

The most dominant algorithm for a local registration is the Iterative Closest Point (ICP) which was developed by Besl and McKay [1992]. The basic idea is registering range images from multiple views of an object based on an algorithm. The main target of the algorithm is to minimize the difference between two datasets, by keeping one fixed (target) and transforming the other (the source) to best match with the target.

The ICP algorithm converges monotonically to a local minimum with respect to the mean square distance objective function. The algorithm computes the transformation parameters by modifying the associations between the target and source points. There are two widely used ICP algorithms, the ICP point to point and ICP point to surface. The first example in Figure 3.1 shows a point to point ICP, where the algorithm obtains point correspondences by iterating searching over the nearest neighboring target points while the second example presents the point to surface algorithm, where the algorithm is searching for correspondences to a whole neighboring surface instead of single points (Bellekens et al. [2015]).

Both versions of ICP algorithm use a linear least-squares optimization problem. An important difference between them is that the ICP point to point algorithm assumes that the neighboring points are created from a known geometric surface and not from random and potential noisy measurements. On the contrary, point to surface

version, relaxes that constraint by allowing point offsets along the surface. Bellekens et al. [2015] also mentions that although ICP point to point algorithm results to less errors, the ICP version point to surface is more precise about estimating the rotation and translation parameters.

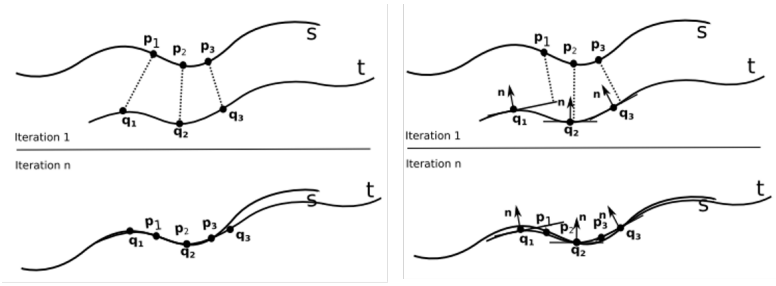

Figure 3.1: ICP algorithm for point to point approach (in the left) and point to surface (on the right)
Bellekens et al. [2015]

The main advantage of the algorithm is that it is independent of the shape representation, it does not require pre-processing of 3D data or local feature extractions and it can handle a reasonable amount of normally distributed noise to data. The main disadvantage is that ICP algorithm is that although the results are quite accurate for densely sampled surfaces, in cases of not a significant overlapping between the views, the results are deteriorated with outliers (Trucco et al. [1999]).

3.2 MODIFICATIONS OF ICP ALGORITHM

Although the algorithm is quite efficient, throughout the years lots of its limitations have been overcome. The ICP algorithm was used as a base and modified several times for improvements. The Iterative Closest Compatible Point (ICCP) algorithm by Godin et al. [1994] differs from ICP as it sets a constraint during the registration. The constraint is about selecting potential matches between pairs of points based on a similarity measure derived from the intensity information. Only pairings of points that satisfy a specific compatibility function are accepted. Robust ICP (RICP) by Trucco et al. [1999], is another modification of ICP algorithm for registering and finding correspondences in 3D point clouds but having significant amount of missing data. The robustness of the algorithm is due to a Least Median of Squares regression (LMedS). More specifically, the LMedS is used within the algorithm and gives the opportunity to use a dynamic translation estimation based on data exempted from outliers. RICP performs iterations and searches for neighboring sets of points rather than finding the closest point on a surface and as it is not including calculation of vectors or derivatives it is applicable to any shape (Trucco et al. [1999]). The basic difference in the Trimmed ICP by Chetverikov et al. [2002] is the use of the Least Trimmed Squares (LTS) approach in many major aspects as to dealing with outliers or shape effects or for partial overlapping for estimating the transformation parameters. The basic theorem is that it converges monotonically

to a local minimum with respect also to the trimmed mean squared error of an objective function.

3.3 PREVIOUS WORK FOR REGISTRATION

As it is already presented in a next section, the ICP algorithm and its modifications uses two different distance metrics, the point to point distance implemented by Besl and McKay [1992] which uses the calculation of the Euclidean distance between the respective points and, the point to plane distance implemented by Chen and Medioni [1992] which uses the distance between a point and a planar surface that is created from neighboring points. This section presents different examples of co-registrations that use different implemented methods for the matching.

3.3.1 Mitra algorithm

An example of a previous work related to pairwise registration of point cloud with different approach is the work of Mitra et al. [2004], who proposed a framework, in which registration is treated as a distance minimization between the surfaces created from the source and target point clouds. They developed an objective function, a second order approximant to the squared distance between the two-point clouds. The method presents a stability even in cases when the initial displacement between the two datasets is large. The main target of the algorithm is to find a rigid body transform composed of rotation and translation parameters that bests aligns one dataset to match the other. The distance between each element of one dataset to the other, is approximated by the sum of distances between the pairs. The algorithm is looking for the rigid transform that minimizes the residual distance between the transformed and the target data.

The quality of the error metric is determined firstly by the degree of how accurately the error metric reflects the distance between the two datasets and secondly, by the validity of the distance approximation not only to a single point but to a neighbor around it. In contrast to ICP algorithms, Mitra et al. [2004] used second order square distance approximants in the scheme, achieving better convergence properties. Generally, they posed the registration as an optimization problem over the space of rigid transformations by minimizing the error distances between the transformed point cloud to the surface created from the other point cloud. The minimization of the error depends on the accuracy of the squared distance function. The algorithm uses the squared distance in a way of trying to plane one point cloud to the squared distance field of the other so to minimize the placement error. Although the framework uses an optimization part, the estimation of the quality of the final matching is not examined.

3.3.2 Key-point matching registration

An automated registration of TLS point clouds using natural planar surfaces was implemented by Theiler [2015]. The general idea is to perform the registration us-

ing virtual key-points that are created from an intersection of planar surfaces in the scene as points that correspond to multiple planes can have multiple geometric invariants and thus are more powerful local descriptors (Figures 3.2 and 3.3). The planes are detected in the dataset with the RANdom SAmple Consensus algorithm (RANSAC) which is an algorithm that copes well with residuals in the datasets and they are fitted using a least squares estimation. As TLS include a vast amount of data, planes can be determined with a high accuracy leading also to well-defined tiepoints. Having two sets of tiepoints in two different scans, registration is performed by looking for the best solution that preserves the geometric configuration of the biggest set of tiepoints.

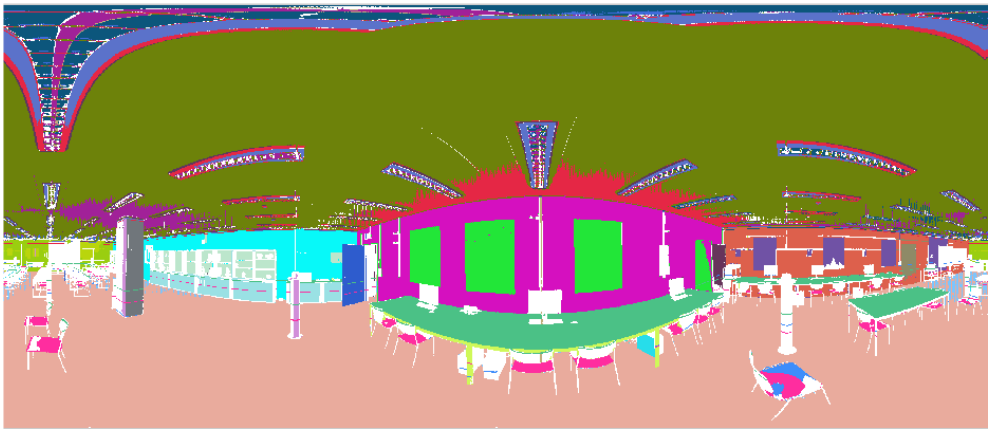

Figure 3.2: Extracted planes in an indoor environment
Theiler [2015]

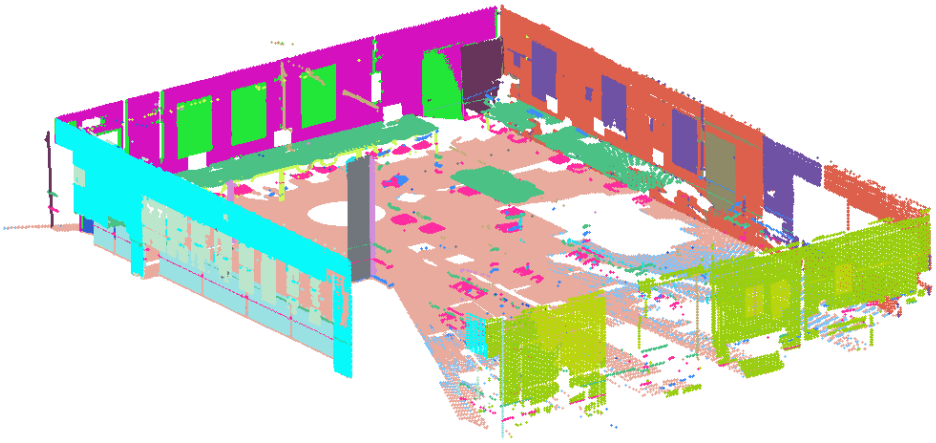

Figure 3.3: Extracted planes in the 3D space in an indoor environment
Theiler [2015]

The quality of the algorithm is evaluated only based on the fraction of points in the source point cloud that can match in the target point cloud and the majority of the faulty registrations occur due to symmetry of the scenes, fact that is eliminated by extracting more planes per scene as a bigger number of planes leads to an increase in successful registrations.

Moreover, Theiler [2015] presented a new framework about a globally consistent registration of multiple point clouds. The whole framework is divided into two parts, a first coarse registration followed by a second fine registration. A first local

initial alignment for all scans is crucial in order to achieve a final successful global refinement. Each part starts with a pairwise registration and ends with an attempt to perform a global alignment across all scans.

The algorithm that is used is a combination of ICP and the global algorithm of Lu and Milios [1997]. As the pairwise registration can find more than one correct solutions, the algorithm aims to filter all the pairwise registrations in a way to form a globally consistent network. Coarse registration uses only a set of corresponding points whilst the fine registration uses a larger set or the whole point cloud. Moreover, if coarse registration is performed correctly it creates a precise input for the fine registration. A pairwise coarse registration finds pairwise alignments in different scans while fine registration must find correspondences between all scans. On the other hand, global fine registration minimizes the noise in transformation parameters by distributing the residual errors that result from pairwise registrations while the global coarse registration weed out the wrong transformation parameters. The overall goal of the work is to register different scans into a common reference system and the framework is said to be applicable to real world data-sets even in cases with a small overlap between the scenes. Lastly, the evaluation of the quality of the output is calculated based on the number of overall success rate by counting the number of scans that are correctly aligned and for verifying the accuracy of the alignment, the mean position error and the mean orientation error are computed.

3.3.3 Point cloud registration using 2D images

A general definition of 2D image registration is the process that aligns one image to a second image of the same scene but acquired in another moment or by other sensor and correlation-based methods are used as similarity metrics (Le Moigne et al. [2002]).

Lin et al. [2017] proposed a method that transforms a 3D point cloud into 2D bearing angle images as registrations with 2D features can reduce computation complexities by using the 2D image matching. A bearing angle image is the gray level image composed from the angle between the laser beam and the vector from a point to its consecutive point (Figure 3.4).

Bearing angles can be used to point out discontinuities of depth and changes of directions in point clouds. After having the images, a 2D feature based matching method is used to find the matching pixel pairs between two images. The matching is computed using the Euclidean distance of two feature vectors. The next step is to check those pixel matchings and filter them so to keep only the correct correspondences. After having the correct 2D correspondences, they are converted back to 3D correspondences. 3D correspondences are further used in a least squares approximation so to create the optimal transformation matrix.

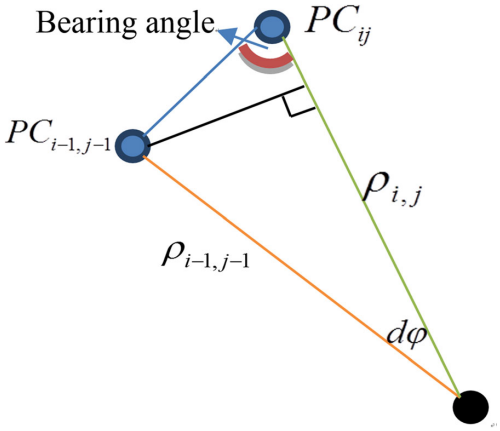

Figure 3.4: The gray level of a pixel of a BA image is defined as the angle between the laser beam and the vector from the point to a consecutive point

A comparison with the ICP algorithm proves that since the algorithm finds the corresponding points without iterative process, it makes it significantly better than the ICP based algorithms as the computation cost is significantly less. However, the precision is not better than the ICP algorithm as filtering does not always work properly resulting to incorrect correspondences to be included.

Christodoulou [2018] also implemented an image-based method for a pairwise registration using mobile laser scanned point clouds. The implemented technique uses the attributes of 3D points to generate and match 2D projections, by using a correlation instead of matching in 3D. The reason is that when point clouds are converted into images and therefore the images are matched, the method is independent of the number of 3D points which is huge but relies on the number of pixels that is smaller, resulting to a less time efficient method. The noise of the point clouds was reduced by computing the local density of the points and the degree of closeness of points to their neighbors characterize it as part of the dataset or not. Using a principal component analysis (PCA), normal vectors are computed, as they are necessary for the extraction of 2D images from 3D point clouds. Using orthogonal projections instead of perspective projections, nine types of images are created for each pair of dimensions XY, XZ, YZ, based on nine different attributes with density, intensity, gradient of intensity, depth, gradient of depth images to be only some of them (Figure 3.5).

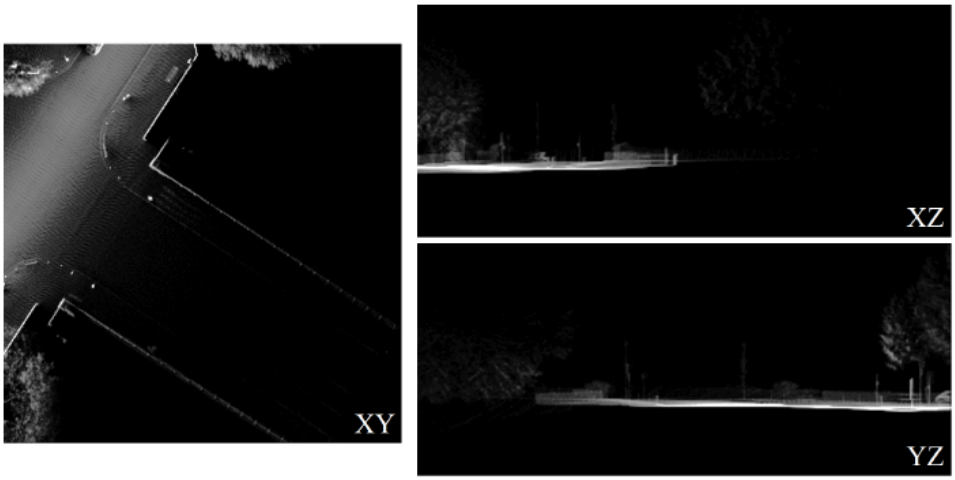

Figure 3.5: XY, XZ and YZ extracted planes from 3D point clouds (Christodoulou [2018])

The creation of different images was done in order to increase the confidence level of the results. A template matching technique based on cross correlation was used for the pairwise registration as different values of brightness exist in images due to different perspectives of view during the recording. Having the result of the template matching, an array with the similarity values, per each projection, two transformation parameters can be calculated per time. Having all the transformation parameters, Christodoulou [2018] uses the equation:

$$matchlocation_p = match_a, match_b \tag{3.1}$$

where:

- p indicates each projection
- a indicates the first axis of the projection
- b indicates the second axis of the projection

to calculate the space coordinates from the image coordinates and to put it simply, to go from 2D to 3D again and the pixel units are converted in real units by multiplying with the respective pixel size. The last part of this research was about finding an optimal solution and evaluate the results. A threshold value was set in order to filter the less accurate results from the template matching.

Moreover, the similarity was double checked using different methods to be in the same image location and in different case the result is again judges as non-reliable and it is not taken into consideration. Lastly, the final criterion for the quality evaluation is the number of pixels with the highest values in the same image. In cases where more than one pixel has high values in an image, its difference with the second pixel that have a high value must be above a threshold so to be judged as a reliable result. Finally, the result of the work proved that results with high quality require a significant overlap between the point clouds and corresponding

objects between two different point clouds must be distinct in pairs of the 2D projections.

Another example of automatic registration is the work of Parmehr et al. [2012] who presented a hybrid intensity-based approach that utilizes both statistical and functional relationships between images and especially in cases where images are registered with 3D point clouds acquired from LiDAR. In their implementation optical imagery is used as the moving image and a Digital Surface Model (DSM) and intensity information from LiDAR data create two individual gray-scale fixed images. A multi-resolution tactic based on the Gaussian pyramid is adopted to accelerate the process but also reserve the robustness. The maximum value of the similarity value is found in the image pyramid with a search from the top to the bottom and results are further used to set values for each next level of the pyramid. Finally, the similarities are calculated for every pair of transformation parameters between the fixed and moving images and the optimal estimation is achieved when the maximum similarity value is found through an optimization procedure.

3.4 A STATISTICAL EVALUATION OF REGISTRATION METHODS

Gümüş et al. [2017] presented a different work, a statistical study of the accuracy of different registration methods used for co-registered scans acquired from different stations. A main part of the research was about analyzing variances in order to estimate the existence of statistically significant difference between coordinates of points acquired from different registrations, a special target-based registration, a specific feature point registration and a surface registration, all of them based on ICP algorithm. The comparison was implemented using the t-student test and a collection of statistical models, an Analysis of Variance (ANOVA). The t-student test is used for determining the significance of differences between two average values in the statistical analysis.

In cases where the differences in coordinates are known, the test is about analyzing whether there are significant differences between the true coordinates (acquired from a total station) and the values obtained from the registration methods. A further step is to test each dataset for an ANOVA analysis but only if there is a normal distribution and homogeneous variances between the datasets. The results of the research used so to prove that the coordinate differences are within the predefined limits of measurement accuracy and the t-test revealed that the differences are consistent. The main conclusion is that the target-based registration method results to an accuracy more realistic than the other methods and the surface-matching method brings better results in comparison to the feature point registration. The whole work can be considered as a generic statistical evaluation of different co-registration methods and it can be used as a preliminary step of the current work as the statistical components give valuable insights about the quality of an output.

3.5 SUMMARY

Various methods have been implemented for different cases of co-registration between point clouds. Different approaches that were analyzed in this chapter give a good insight about different registration characteristics. It is important to be mentioned that the majority of the works deal only with the functional model of the registration and limited research had been done about the stochastic part that gives insights about the quality of the functional part. Consequently, it is noteworthy that the quality of the results is hardly addressed. Although the technological development, the modern equipment and the automated processes that have been developed in the field of engineering, the actual evaluation of the results is not yet elaborated in depth and little attention had been given to test the outputs of a registration for satisfying predefined quality demands.

4 IMPLEMENTATION, TOOLS AND DATASETS USED

This chapter is organized as follows: The first section describes the tools, datasets, hardware and software that were used in order to implement, analyze and present the result of this research. The second section provides information about the implementation of the approach based on the theory that has been introduced.

4.1 TOOLS AND DATASETS USED

For the implementation of this work, Python scripts have been developed. The scripts have as input response images, the result of a co-registration between point clouds. As the main concept has a generic target, the algorithm can also take as input, images from other datasets.

4.1.1 Software

The method will be implemented using the scientific environment of Spyder with Python 3.7 combined to some software libraries suitable for point clouds, image processing and statistics like lastools, laspy, imageio, shapely, descartes, plolty, matplotlib, lmfit, numpy, scipy.

- Lastools: It is a software suitable for LiDAR processing. It is used for decompressing .laz files into .las files in order to be readable in Python.
- Laspy: It is a library in Python for reading and modifying LiDAR files. It is used for finding the densities of the MLS and ALS data for each tile.
- Imageio: It is a library used for image processing. By using this library, the images are readable and usable.
- Shapely: A BSD-licensed Python package, suitable for manipulation and analysis of geometric objects as ellipses.
- Descartes: It is a platform that is used in combination with shapely for creating geometric objects as circles and ellipses.
- Plotly: It is an online tool that gives the opportunity of developing visualizations that are interactive to the user, so to change the zoom or the perspective view of the output and achieve the best representation of the diagram.
- Matplotlib: It is a package used for plots and visualization of the 2D and 3D results.

- Lmfit: It is a package that provides a high-level interface for line fitting problems and optimization. Models wrap well known functional forms as Gaussian. The models provide methods in order to estimate the best approximation of fitting parameters to the given initial values. It is used for determining the best approximation of fitting a Gaussian line to the pixel values.

- Numpy: It is a package for scientific computing when using python. Among others, it makes manageable the use of multidimensional arrays, that in this work case are the images. It is used for calculating the mean values in the arrays and in .las files.

- Scipy: It is a library used for the statistical analysis of the results. Using the package stats that is include in scipy, the tests about checking the normal distribution of values are implemented.

4.1.2 Hardware

For the execution of the tests and the analysis, a computer with Intel Core i7 processor, RAM memory of 16GB and CPU 2.60 GHz was used.

4.1.3 Datasets used

The datasets used are obtained from an image based co-registration. 2D Response images, the results from the integration of different point clouds are used for the tests and the analysis. Point clouds are collected during the mobile laser scanning process using MLS and ALS techniques. The recorded point clouds are stored in tiles of 50m by 50m and each tile is used for the creation of the respective 2D input images with 500x500 pixel size that are used as input in the template matching. After performing the matching, a 2D response image containing the matching scores is extracted with 61x61 pixel size.

Point clouds and consequently images depict some regions of Eindhoven in the Netherlands. The term MLS and ALS scanned points clouds implies LiDAR data. MLS data are collected with an HDL-32E Velodyne scanner and are provided from the company Cyclomedia Technology B.V. An HDL-32E Velodyne scanner has a 360°horizontal field of view and has a measurement range up to 70 meters and accuracy of +/- 2cm. It utilizes 32 laser pairs and it has the potential to scan and generate approximately 700.000 points per second (Velodyne 32-E High Definition LiDAR Sensor [2019]).

ALS data is also provided from Cyclomedia Technology B.V. and acquired from a Leica CityMapper. CityMapper is a hybrid airborne sensor combined with a LiDAR system that provides 3D point clouds with a sampling density of +/- 6 points per square meter.

4.2 IMPLEMENTATION

This section describes the main parts of the implemented method, based on the theoretical parts of the previous chapters.

The analysis is performed using 2D response images with 61x61 pixel resolution. Response images are extracted by performing a template matching between the input images with size 500x500 pixels referring to 50*50m tiles, for different attribute types as density, color and depth for four different regions in the city of Eindhoven, in the Netherlands. More specifically, 477 response images are obtained for the region of the city center of Eindhoven, 480 for a park in the city, 742 images are related to the stadium in Eindhoven and 718 for a specific neighborhood, a former industrial park in the Eindhoven district called Strijp (Table 4.1).

Response images of the city of Eindhoven per region	
Region	**Number of response images**
City center	477
Park	480
Stadium	742
Strijp region	718

Table 4.1: Response images used for the implementation

The response images are analyzed as matrices and the pixel values are used as they contain the important information of the matching. A python script is used in order to test the distribution of the pixel values. If the distribution of the values follow the normal distribution in both dimensions of the images, the images are further used for the analysis. A normalization of the image values is following and a statistical analysis of the images gives insights about their characteristics. Based on the statistical measures of the images, conclusion about their quality are drawn and relevant weights are assigned to each of them. An analytical description of all the individual steps are further discussed in the next chapter.

4.3 DIFFERENT DENSITIES BETWEEN MLS AND ALS TECHNIQUES

Response images are extracted from point clouds acquired from MLS and ALS techniques. It is known that different scanning equipment generate different point clouds regarding their densities. As a result, it is important to present the different characteristics of MLS and ALS point clouds.

Typical examples of points clouds with different densities are shown in Figure 4.1. The first point cloud is generated using an MLS technique and the number of scanned points is 12,869,188 while the second one is scanned with an aerial scanner and the number of points is 53,588. The respective extracted images are shown in Figure 4.2 as well as the response image from the template matching. The first image has more discrete bright parts as the point cloud is richer while the second image has less distinguishable differentiation in lines as the ALS point cloud is sparser.

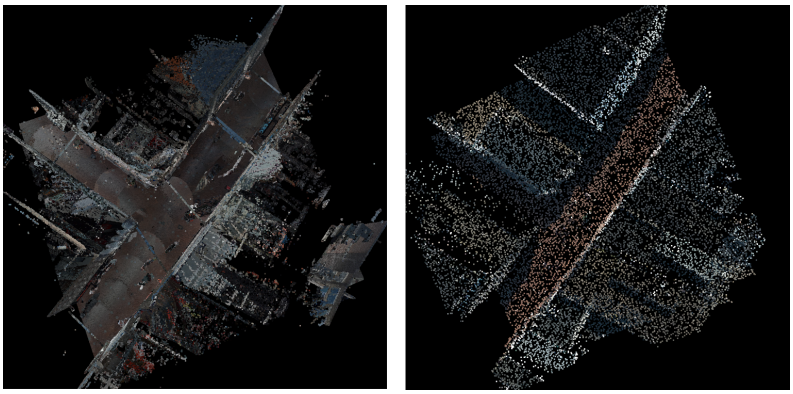

Figure 4.1: MLS point cloud is depicted on the left and the respective ALS point cloud is depicted on the right. The amount of points that each point clouds includes is 12,869,188 and 53,588 respectively.

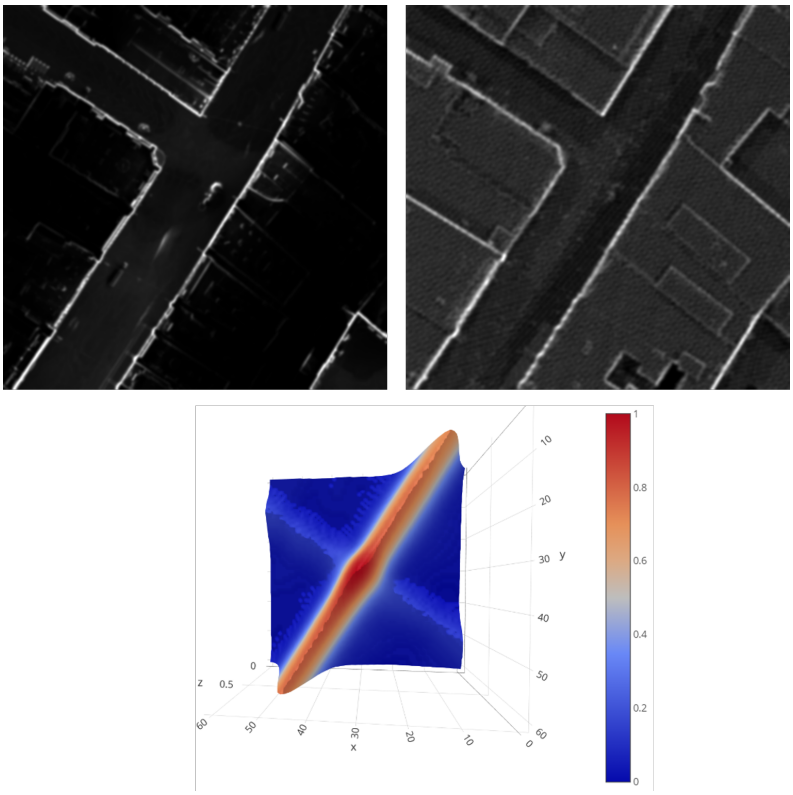

Figure 4.2: At the top the extracted images from MLS (left image) and ALS (right image) point clouds are presented while at the bottom it is presented the response image after performing the template matching technique.

In the Table 4.2, the densities of point clouds in the tested regions in Eindhoven are presented. The numbers depict the average number of points per each region. Point clouds generated using MLS techniques are significantly bigger compared to point clouds acquired from ALS techniques which are quite sparse as millions of MLS points are compared to thousand of ALS points in all cases.

Densities for MLS and ALS point clouds in average		
Region	MLS points	ALS points
City center	613,410	71,140
Park	3,371,052	80,280
Stadium	2,823,568	82,524
Strijp region	2,746,082	84,998

Table 4.2: Average number of points for MLS and ALS techniques in each region

5 ANALYSIS

This chapter presents the analysis of the resulting response images of image based co-registration between point clouds acquired from MLS and ALS techniques. The distribution of pixel values of response images acquired from different attributes of an image are analyzed in order to determine important parameters for the images. Precision and reliability, two significant indicators are addressed in order to approach the term of quality. Additionally, the shift parameter is also calculated, giving us the opportunity to combine response images that belong to neighboring tiles for their similarity.

5.1 IMAGE ANALYSIS

In a registration approach, the quality of the solution is evaluated based on the input image after applying the estimated transformation parameters resulting to the respective response image (Ripperda and Brenner [2005]). The response image per attribute type is with other words the result from the template matching between two input images of the same attribute type, extracted from different point clouds but referring to the same area. For the evaluation response images from different attributes are analyzed. The attributes that are used are:

- the color attribute
- the depth attribute
- the density attribute

Color attribute:

The color attribute of the input images occurred from the LiDAR data in combination with the natural colors that are processed in 3D point cloud data from high definition panoramic images acquired at the same time with the point clouds. As images are RGB images, every pixel is accompanied by a triplet of numbers, one for each band. The final image that is used is occurred by a cross correlation technique of the RGB colors. More specifically, values are generated by summarizing all pixels of all bands in pairs and afterwards normalizing them based on the fact that the result is equal to 1 if all pixels are white.

Depth attribute:

In 2D input images, the depth attribute depicts the values of the points in the 3rd dimension. The closer the object is located to the laser scanner, the smaller depth value has in the image and vice versa. Images acquired from the depth attribute are useful as they avert faulty registrations of identical objects.

Density attribute:

Density attribute contains information about the total amount of points that exist in this specific 2D image. It is a useful attribute as big objects become easily distinguishable as there are multiple scanned points belonging to them.

5.1.1 Response images acquired using the same attribute of density

Firstly, as a typical case, Figure 5.1 shows the input images for the co-registration at the top, the response image in 2D at the bottom and left side of the image and the distribution of the pixel values using a representation in 3D at the bottom and right part of the image. The 3D representation is achieved by using as third dimension the value of each pixel and by this value the respective bar is erected (Figure 5.2).

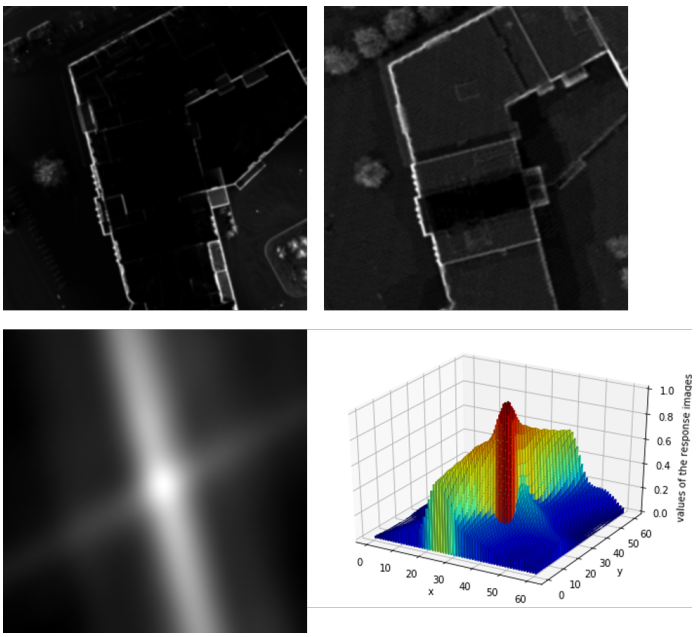

Figure 5.1: A response image using the density attribute. At the top of the image: two images extracted from two different point clouds referring to the same area. At the bottom: on the left side is presented the 2D representation of the response image and on the right the respective 3D representation of the response image

The response images are presented using pixel units and the resolution is 61*61 pixels. The values of the pixels vary from 0 to 1. Both input images in Figure 5.1 have bright and dark pixels that can be seen. The brighter pixels indicate high values of matching (close to 1) during the matching procedure and dark pixels indicate smaller values (close to 0). Higher values of matching point out a better matching and the opposite occurs for the smaller values.

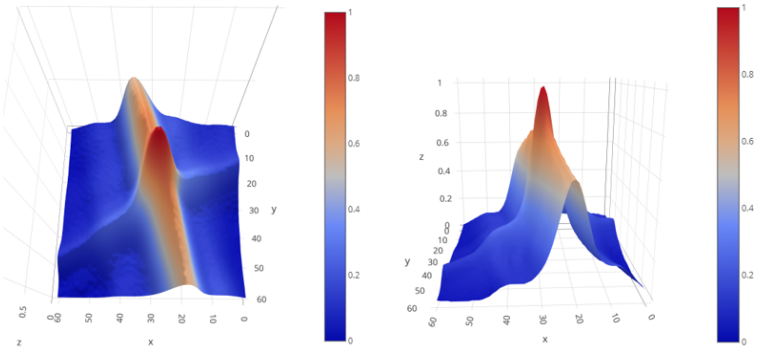

Figure 5.2: The 3D representation of the response image from different perspective views

Although the response image in Figure 5.1 is extracted from input images that use the same attribute of density and they are referring to exact the same region, various of differences exist between them. Corresponding pixels have quite different values. For instance, the first input image at the top depicts the footprint of the building with brighter pixels than the second one while the second image depicts trees that are not visible at all in the first image.

5.1.2 Comparison of response images acquired from different attributes

In different attribute types, the dark and bright parts of the image denote different characteristics. For instance, for the attribute type of density, the disparity between dark and bright parts of the response image are due to different number of recorded points. The fewer points exist, the brighter is the corresponding part of the image. Another example is the depth attribute, where the brighter parts of the image correspond to scanned points with a smaller depth and consequently a smaller distance from the scanned point to the laser scanner.

The sequence of images (Figures 5.3 , 5.4, 5.5 and 5.6) show the pair of input images at the top and the respective resulting response image in 2D and 3D at the bottom for different attribute types but for the same scene as in Figure 5.1. Although the response images are referring to the same area, the results are completely different.

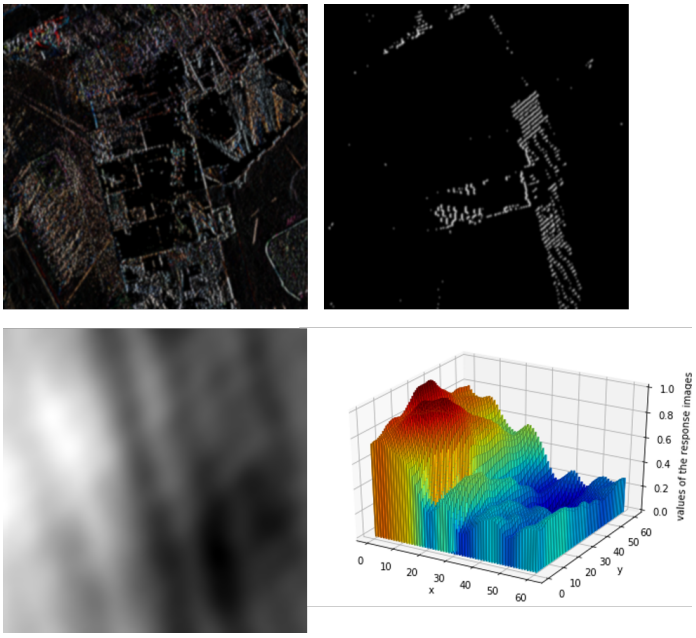

Figure 5.3: A response image using the color attribute in dx orientation. At the top of the image: two images extracted from two different point clouds referring to the same area. At the bottom: on the left side is presented the 2D representation of the response image and on the right the respective 3D representation of the response image

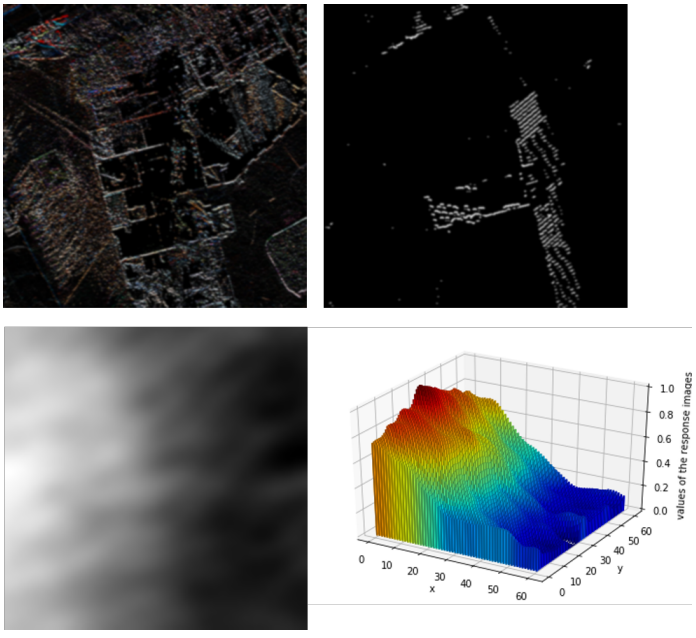

Figure 5.4: A response image using the color attribute in dy orientation. At the top of the image: two images extracted from two different point clouds referring to the same area. At the bottom: on the left side is presented the 2D representation of the response image and on the right the respective 3D representation of the response image

Each attribute of an image is suitable for only some regions with common characteristics and less representative for others (Table 5.1). For instance, in a specific case of a building environment, the density attribute type gives a better result for the building blocks compared to the color or depth attribute. Walls and general big ele-

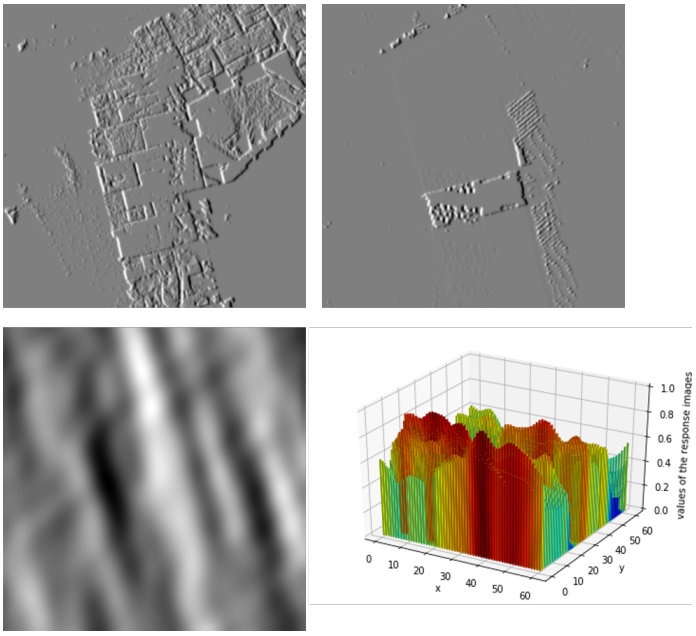

Figure 5.5: A response image using the depth attribute in dx orientation. At the top of the image: two images extracted from two different point clouds referring to the same area. At the bottom: on the left side is presented the 2D representation of the response image and on the right the respective 3D representation of the response image

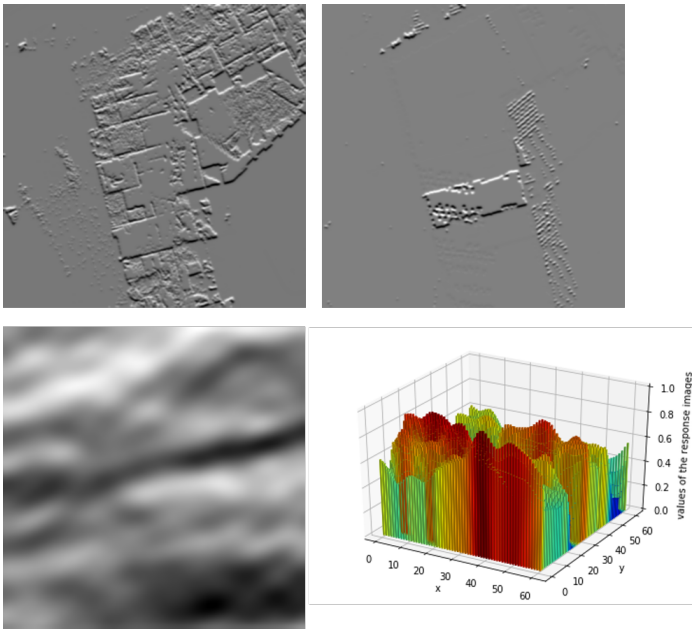

Figure 5.6: A response image using the depth attribute in dy orientation. At the top of the image: two images extracted from two different point clouds referring to the same area. At the bottom: on the left side is presented the 2D representation of the response image and on the right the respective 3D representation of the response image

ments with constant structure are easily distinctive in the images as their structure causes lots of points to fall into the same bin of the image (Someren [2016]).

Different attributes of the images	
Attribute of the image	**Suitability**
Color	Vegetation
Depth	In order to avert faulty registrations of identical objects
Density	Objects with constant structure (e.x. buildings)

Table 5.1: Response images per attribute type and suitability

In general, density is an important and usable attribute in image processing for an urban environment as features with long and thick characteristics are represented with high amount of points and are easily distinguishable. On the contrary, the color attribute gives better representation for regions that do not have building structures but vegetation.

5.2 METHODOLOGY OVERVIEW

Except from the visual indications that a response image gives, a statistical analysis is performed as it gives more robust indications about the data. The distribution of the pixel values in both dimensions is checked and conclusions are drawn based on their statistical analysis. Normal distribution is proved using statistical tests with the aim of gaining knowledge about the characteristics of the response images.

Figure 5.7 presents a general overview of the main parts of the developed method. 2D response images from different attribute types are used as input data for the analysis.

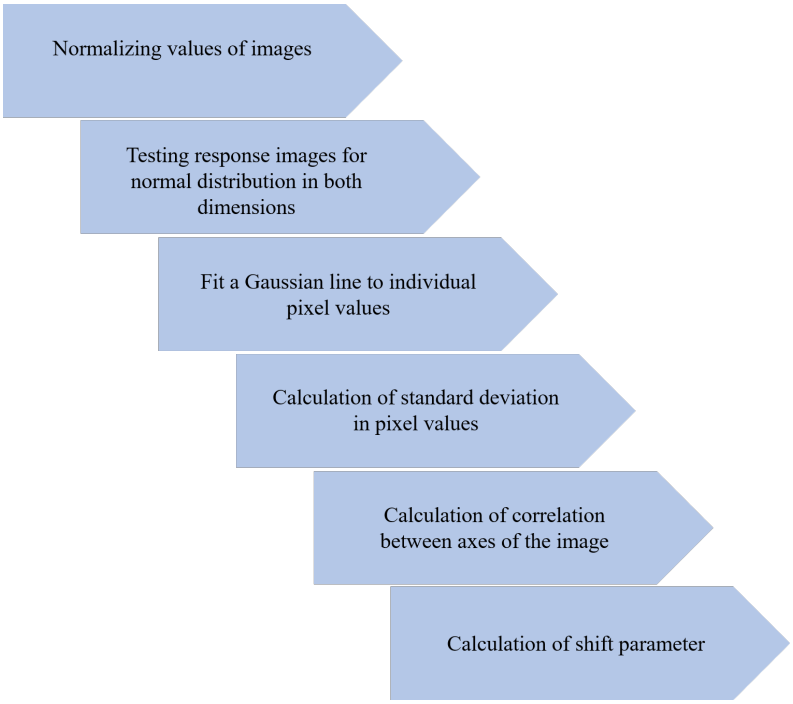

Figure 5.7: Overview of the developed methodology

5.3 STATISTICAL ANALYSIS

The disturbance from the perfect alignment changes the values of the response image, creates more than one peaks or shifts the peak from the center of the image. Various statistical measures exist as mean, median, variance, standard deviation, co-variance, skewness and kurtosis in variety of scientific researches as well as in image processing (Kumar and Gupta [2012]).

Mean is the most typical example of statistical measures. Mean values are used in geometry and analysis. The arithmetic mean, which is often called 'averaging filter', operates on an image by calculating the average of all pixels. It can be used to reduce different types of noise in an image, as Gaussian, uniform or Erlang noise. Another widely used measure is the standard deviation of the values of an image. It is a measure that characterizes the variability and diversity of values of an image. It expresses how much the values deviate from the mean value. A low standard deviation indicates values of pixels close to the mean value while a high standard deviation indicates a spread over a large range of values. Hence, the analysis of the response images will be implemented using such statistical measures.

5.3.1 Normal distribution in 2D

There are different tests that can be performed in order to check the normal distribution of samples. The employed test is the Kolmogorov–Smirnov test (K–S test or KS test). It is a non-parametric test of the equality of one-dimensional probability distributions. Distributions in both axes of the images are tested separately. For both cases a probability value is extracted from the employed test and it is compared with a predefined significance level.

The selected significance level is 0.5%. Every extracted probability value is compared to the significance level in order to decide the acceptance or rejection of the null hypothesis that the distribution of pixel values is normal. Only when the probability value is greater than the significance level the result is statistically significant. Response images that satisfy both tests for both axes are further used.

This double check is useful as it implies that the response image follow the normal distributions both horizontally and vertically. In different cases it is withdrawn as it is considered important to have indications about both axes.

However, it is important to be mentioned that in examples of co-registrations with limited data where every piece of information is valuable, limited indications can also be obtained from response images that follow the normal distribution only in one from two axes. In this latter case, the conclusions that can be drawn are less accurate as there is a less detailed parameter definition.

5.3.2 Normalizing the images

More specifically, the first part of the analysis of the response image is performed in x and y and later the individual results are combined. The distribution of the pixel values is analyzed rather than the individual values. In order to do this, the whole response image, with size 61 pixels horizontally and 61 pixels vertically is transformed. The response image is treated as a matrix. Firstly, for each row and each column the mean value is calculated based on the typical equation for calculating a mean (μ):

$$\mu_{row} = \frac{\sum_{i=1}^{61}(p_r)}{61} \tag{5.1}$$

$$\mu_{column} = \frac{\sum_{i=1}^{61}(p_c)}{61} \tag{5.2}$$

where:

p_r indicates all the pixel values per row and p_c indicates all the pixel values per column.

Afterwards, the mean value per row or column is subtracted from all the pixels values of the respective row or column resulting to new arrays. This step is used as pre-processing of the data with the aim of normalizing the images and centering the pixel values so to make them comparable to each other. The following pseudo code presents the different steps that are required in order to normalize the pixel values of the response images.

Algorithm 5.1: How to normalize pixel values for response images

```
create matrix for calculated values per row;
create matrix for calculated values per column;
for every response image do
    for every row of the response image do
        find mean value;
        append it to a new matrix for rows;
        find the mean values of matrix for rows;
        for every value in mean matrix for rows do
            subtract the mean value from each pixel value;
            if the value is positive then
                append the value to the matrix for rows;
                if the value is negative then
                    replace the value with zero;
                    append zero to the matrix for rows;
                end
            end
        end
    end
    for every column of the response image do
        find mean value;
        append it to a new matrix for columns;
        find the mean values of matrix for columns;
        for every value in mean matrix for columns do
            subtract the mean value from each pixel value;
            if the value is positive then
                append the value to the matrix for columns;
                if the value is negative then
                    replace the value with zero;
                    append zero to the matrix for columns;
                end
            end
        end
    end
end
```

A typical example of normalizing an image's values is presented using a smaller image of 10 pixels. Figure 5.8 depicts the calculated mean values (μ) for each row and Figure 5.9 presents the calculated mean values (μ) for each column. The next step is to calculate the general mean of the mean values of rows (μr) and the general mean of the values of columns (μc) which is 0.62 for both cases.

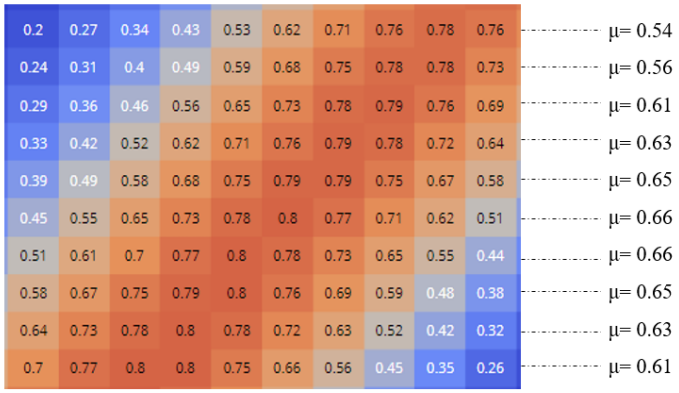

Figure 5.8: Calculated mean values for each row

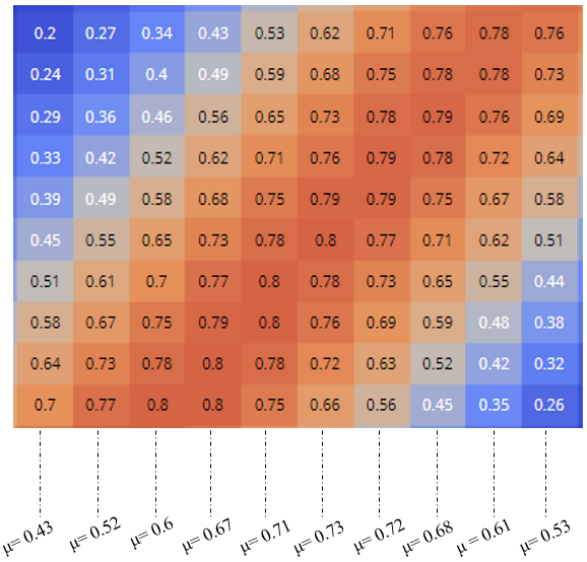

Figure 5.9: Calculated mean values for each column

Figure 5.10a shows the original pixel values while Figure 5.10b shows the values of each pixel having subtracted the general mean of rows or columns. Finally, 5.11 presents the values that are used in the analysis after replacing the occurred negative values from the previous step with zero. It is important to be mentioned that the distribution of the values is not distorted but the values are centralized.

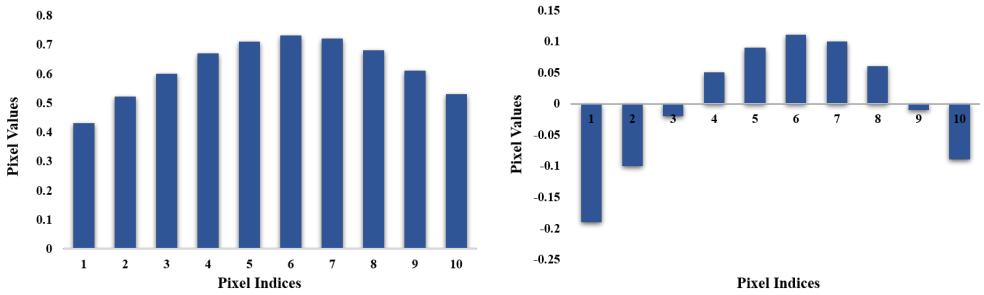

(a) Original pixel values **(b)** Pixel values after subtracting the mean value

Figure 5.10: Pixel values before and after the subtraction of the mean value

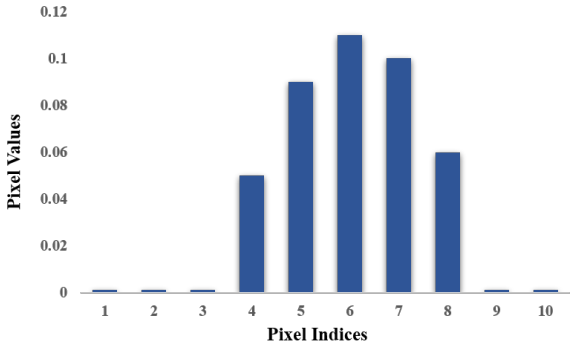

Figure 5.11: Pixel values after replacing the negative values with zero values.

In Figure 5.12 the histograms of real response images ares depicted before and after the normalization. The images at the top depict all the pixel values of the 61*61 response image while the images at the bottom present the normalized histograms of the images after the transformations.

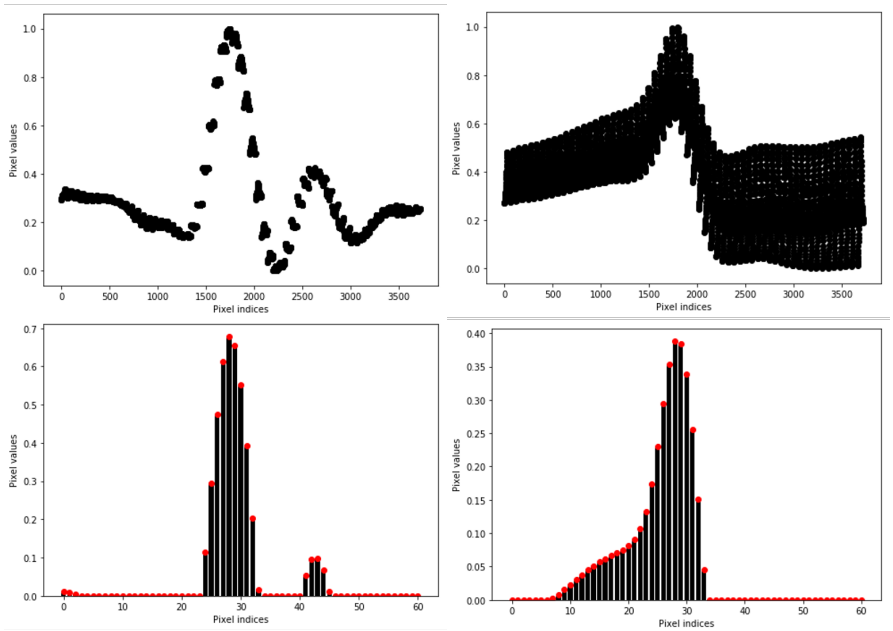

Figure 5.12: At the top the distribution of pixel values in original response images and at the bottom in normalized response images

Normalizing the images' values by subtracting the mean create values that are more uniform and numerically equal, making the algorithms run quickly. The mean value is selected after multiple tests as it gives the best result compared to the maximum and minimum values. It is important to be mentioned that although the values are transformed, the distribution remains unchanged as it can be distinguishable in response images depicted in Figures (5.10, 5.11 and 5.12).

The images are analyzed using pixel units. The size of the pixel is 10cm and each response image with size 61 by 61 pixels is created from the template matching between input images with size 500 by 500 pixels that correspond to 50 by 50m tile in reality. During the template matching procedure, on input image is used as a template and the other as the reference image. However, as the template image must be smaller than the reference image in order to shift over it, every time only the central part of the first input image with size 440 by 440 pixels is iteratively shifted over the second one. Therefore, by 30 shifts in all four directions, a response image with 61 by 61 pixels is generated.

The total amount of response images that are tested is 2417. The next Table 5.2 presents the amount of response images per region that follow the normal distribution after the normalization of their values. The percentages of images that pass the normality test are for the city center dataset 61 %, for the park dataset 59 %, for the stadium dataset 51 % and lastly for the Strijp region 55 %. Although the datasets are referring to completely different regions, the percentages of response images that pass the normality tests do not differ significantly.

Response images of the city of Eindhoven per region		
Region	**Number of response images**	**Number of response images that pass the normality test**
city center	477	293
park	480	287
stadium	742	377
Strijp region	718	391

Table 5.2: Response images per attribute type on the left and the number of them that have normally distributed values for both dimensions on the right

5.4 SUB PIXEL ACCURACY

Using the discrete values for the analysis and the calculation of the standard deviation the best accuracy that can be achieved is equal to the pixel size. As a consequence, the translation parameters are always a multiple of the pixel size. In this specific work, the pixel resolution is equal to 10cm, so it is practically difficult to find translation parameters with accuracy greater than 10cm. However, the result of a matching is not located in a single point but in a single pixel with size 10cm. That makes it clear that the peak point can be located everywhere within these 10cm. Therefore, it is important to investigate if it is possible to perform a sub-pixel accuracy method as it is beneficial for the accuracy of the results.

5.4.1 Interpolation by fitting a polynomial

Interpolation between the individual pixel values is one typical example for achieving a sub-pixel accuracy. Zhang et al. [2009] performed a novel sub-pixel interpolation according to the correlation peak, to gain the final matching position by the principle of parabola interpolation method. However, previous researches proved that fitting a second order polynomial on the values brings poor results and polynomials of higher order fit differently in each individual response image and the lines have significant deviations from the values (Christodoulou [2018]).

Moreover, by fitting polynomials of high degrees over a set of points usually leads to the Runge's phenomenon. It is an oscillation problem at the tails of the line and the greater the degree of the polynomial the stranger the fitted line becomes at the edges. In Figure 5.13 examples with polynomials with 10, 20 and 40 degrees are shown.

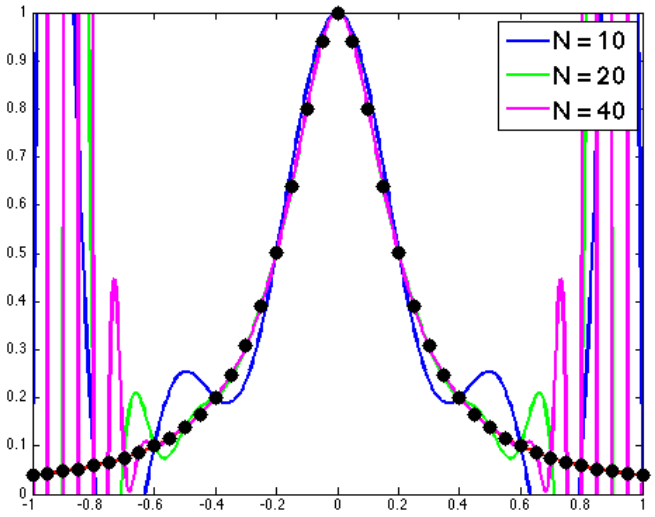

Figure 5.13: Polynomials of different degrees are fitted to the data points. Boise State University [2019]

5.4.2 Interpolation by fitting a Gaussian model

Instead of analyzing the discrete pixel values, a line is fitted on the values of response images that represent the matching score. Every time a line is fitted to the distributions of values per row and column for every response image. As it is already proven that these values around the peak of the response image are normally distributed, a model based on Gaussian or normal distribution line shape is used in order to approach the best approximation of the line to the pixel values. The model that was used is characterized by the function:

$$f(x; A, \mu, \sigma) = \frac{A}{\sigma\sqrt{2\pi}}\, exp[\frac{-(x-\mu)^2}{2\sigma^2}\ ]$$

where:

- A is the amplitude of the distribution of the values
- μ is the center of the distribution of the values
- σ is the standard deviation of the values

In Figures 5.14 and 5.15 red dots indicate the discrete pixels values for the respective pixel index and the blue line is the best approximation of fitting a line. In practice, the best fitting of the line to the discrete pixel values is performed by minimizing the sum of the squares of the offsets. These offsets are the point by point differences between the points and the line. Typical examples of offsets are depicted in Figures 5.14 and 5.15 with yellow arrows.

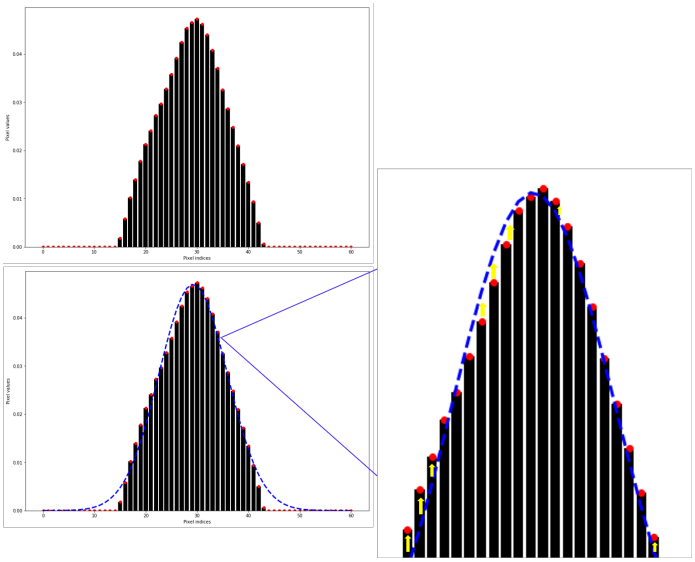

Figure 5.14: Two images on the left present the distribution of pixel values per row. The image above presents the individual pixel values and are pinpointed with red dots . The first image below presents a line fitted to pixel values using a Gaussian model while the second image is a zoomed output. Yellow arrows indicate the offsets between the line and the discrete pixel values that are minimized by the selected line.

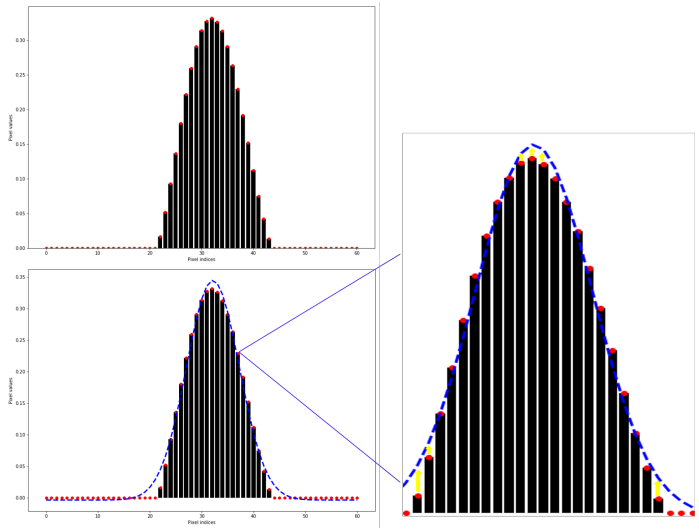

Figure 5.15: Two images on the left present the distribution of pixel values per column. The image above presents the individual pixel values and are pinpointed with red dots . The first image below presents a line fitted to pixel values using a Gaussian model while the second image is a zoomed output. Yellow arrows indicate the offsets between the line and the discrete pixel values that are minimized by the selected line.

Fitting a line to a dataset with points is also equivalent to maximizing a likelihood function with respect to its model parameters by using a least squared regression. A number of fitting lines are applied iteratively until the best one is found. Figures 5.14 and 5.15 give two different examples where the fitted lines can be said that deviate at some locations, but the ultimate target is the estimation of the minimum fitting error.

More specifically, instead of taking only one value as a peak, the maximum value in the response image, multiple neighboring pixel values are considered. Figure 5.16 gives an impression about the pixel values in a small part of a response image around the peak value. By fitting a line, a kind of interpolation is performed as all the neighboring values of the pixels are taken into account and values of sub-pixel accuracy are generated. Consequently, information is also acquired for locations between the discrete pixels and an accuracy greater than the pixel size is achieved.

Of course, there are datasets with multiple residuals and the fitted line is highly sensitive to them. In examples like that, an additional criterion should be adapted in order to test how accurate is the fitted line to the points. For example, in response images with multiple peaks, a new constraint will be beneficial about rejecting the second highest peak compared to the first one. Finally, by fitting a line to discrete pixel values some drawbacks also occur with the most important to be the loss of accuracy as there are values that are neglected with the purpose of finding the line that minimizes the distances between the line and the points. However, the loss of accuracy does not lead to a loss of precision but on the contrary precision is increased as values have smaller deviations between them.

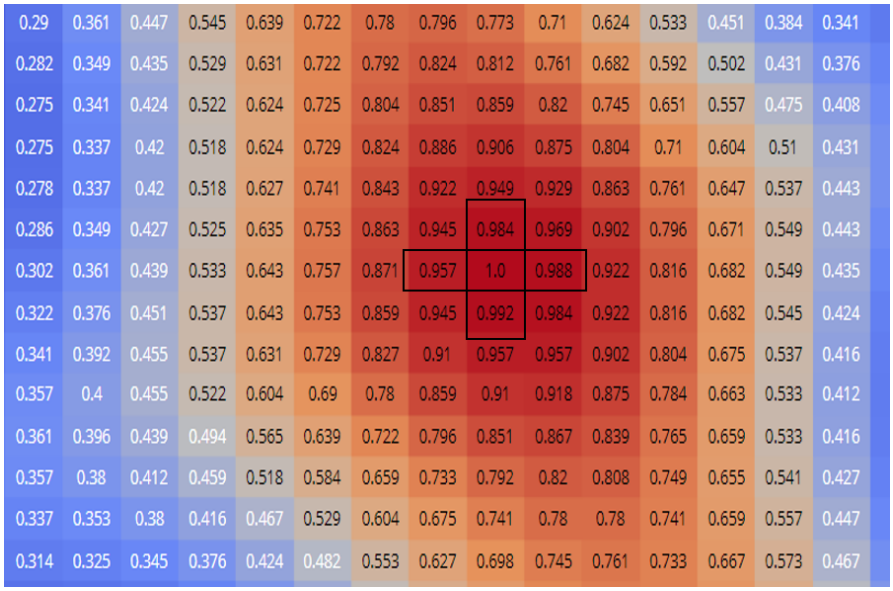

Figure 5.16: Instead of taking only the peak value, all the neighboring high values are considered for the analysis, contributing to a sub-pixel accuracy

5.4.3 Outcome of fitting a line

For every response image, a number of common parameters are calculated in order to take the line that best fits to the pixel values. An amplitude parameter, represents the overall height of the area, or the peak. A center parameter, that best approximates the peak position within the values and a sigma parameter that characterizes the width of the distribution and therefore the distribution of the values. It is also possible to calculate the full width of the distribution at the half maximum value but it is not considered useful for this research.

5.4.4 Calculation of the standard deviation

Standard deviation is calculated from the fitted line in order to have the better possible accuracy. Generally, standard deviation of a one-dimensional data can be thought as the measure of the spread of the probability and by definition, there is a 0.684 probability that normally distributed values fall within the region by -σ and +σ around the mean, in a bell curve. For instance, in the before mentioned response images (Figures 5.14 and 5.15) the calculated standard deviation is 6.8 pixels per row and 5.1 pixels per column as it can be seen in the respective Figures 5.17 and 5.18.

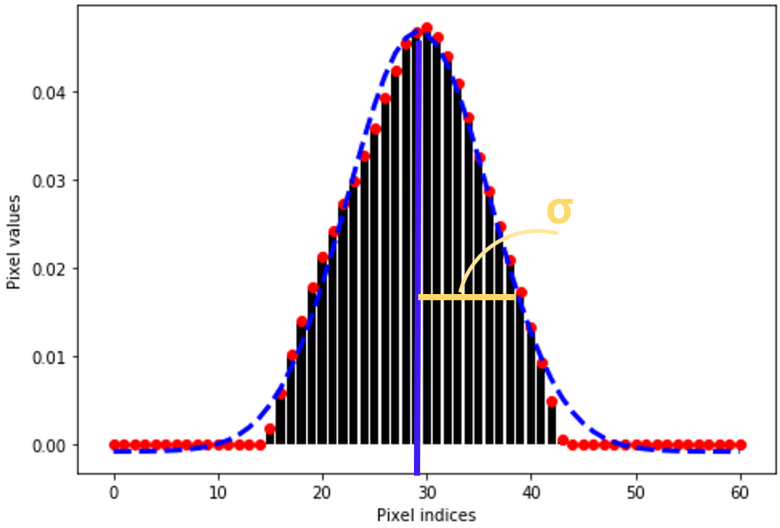

Figure 5.17: Calculated standard deviation from the fitted line for the distribution of pixel values of rows

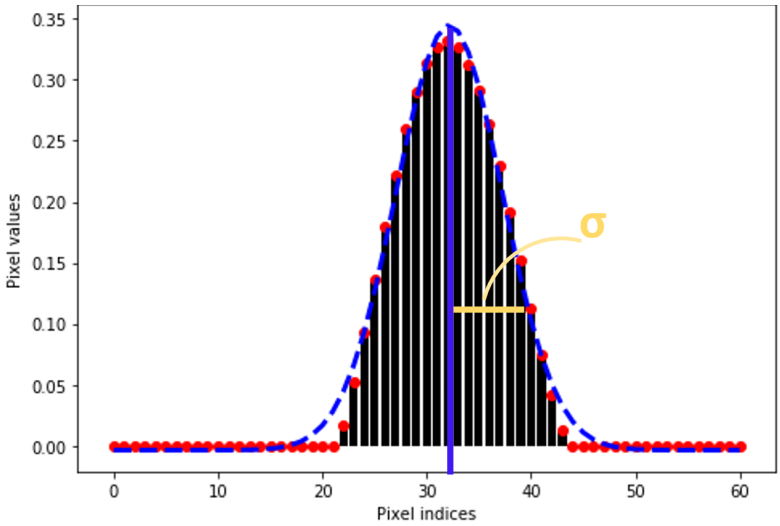

Figure 5.18: Calculated standard deviation from the fitted line for the distribution of pixel values of columns

Although in 1D cases, standard deviation can be calculated easily, in multivariate normal distributions, also called multivariate Gaussian distributions the calculations are quite more complex. A multivariate Gaussian distribution is parameterized by a mean vector and a co-variance matrix which includes the different variances of the dimensions and therefore their standard deviations. In case of 2 dimensions x and y, a bi-variate normal distribution is characterized by the function:

$$f(x,y) = \frac{1}{2\pi\sigma_x\sigma_y\sqrt{1-\rho^2}}\, exp[-\frac{1}{2(1-\rho^2)}\,(\left(\frac{x-\mu_x}{\sigma_x}\right)^2 + \left(\frac{y-\mu_y}{\sigma_y}\right)^2 - 2\rho\left(\frac{x-\mu_x}{\sigma_x}\right)\left(\frac{y-\mu_y}{\sigma_y}\right))]$$

where:

- σx is the standard deviation in x axis

- σy is the standard deviation in y axis
- μx is the mean value in x axis
- μy is the mean value in y axis
- ρ is the correlation between x and y axes

Therefore, a two-dimensional standard deviation is a two-dimensional summary of two-dimensional data. In the ideal case of a normal distribution, a typical way to visualize the standard deviation in 3D is by plotting a circle which is centered on the mean values of distributions in both axes and has a radius of one sigma (Figure 5.19).

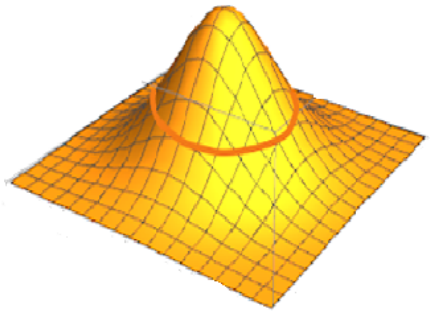

Figure 5.19: A perfect normal distribution where a circle perfectly fits.

In the reality, the datasets are not perfect and the standard deviations in two dimensions are circular but they are best described by ellipses, the confidence ellipses. The shape of an ellipse is defined by the semi major axis a and semi minor axis b as they are presented in Figure 5.20. The orientation of the ellipsis is determined by the correlation between the axes and it is described in a next section.

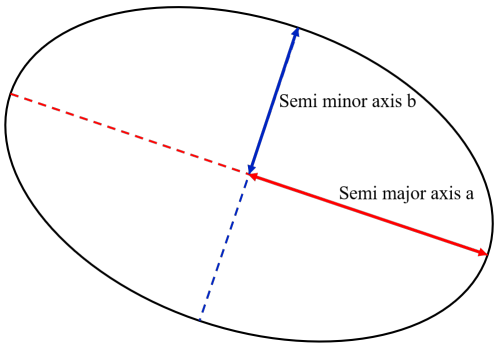

Figure 5.20: Standard deviation in 2D is described by an ellipsis.

5.4.5 Outcome of calculating the standard deviation

By calculating the standard deviation of the pixel values for each response image for both dimensions, conclusions are created for the actual deviation among the values. Response images that have small deviations among values are more precise. Additionally, small values in standard deviation creates sharper peaks in the distributions while bigger standard deviations create more flattened peaks. A good estimation of the peak and therefore the line that is fitted to it leads to an optimal estimation of the transformation parameters. Moreover, standard deviation values can be used as a good indicator in order to classify or filtering the datasets. Filtering can be used to remove images that demonstrate a noisy behavior in their values. Lastly, by classifying the response images, that are results from a local pairwise co-registration, relevant weights are assigned to them and they are becoming valuable parts of a future global registration.

5.4.6 Distributions with different characteristics

Different examples of Gaussian distributions are presented in Figure 5.21. The left figure shows a a standard normal Gaussian distribution with zero mean and co-variance matrix Cov=I, a 2x2 identity matrix. The middle figure presents a Gaussian with zero mean and co-variance matrix Cov=0.6 I and the rightmost figure shows a distribution with zero mean and a co-variance matrix Cov=2 I.

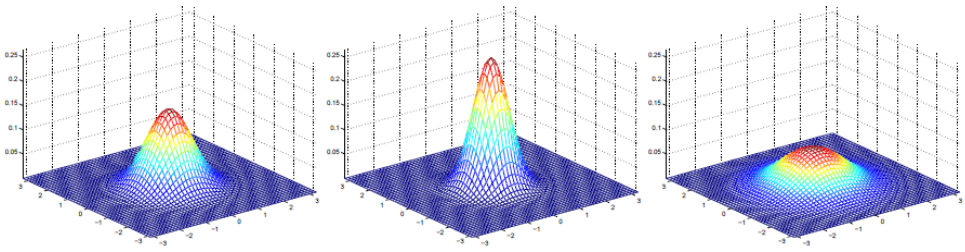

Figure 5.21: Examples of Gaussian distributions with co-variance matrices I, 0.6I and 2I (Ng [2000])

It is clear from the images that as the co-variance matrix becomes larger, the Gaussian is more spread while a smaller co-variance matrix leads to a more compressed representation. More examples, with different co-variance matrices can give a better insight (Figures 5.22 and 5.23). In these examples the Gaussian distributions have zero mean in both axes and the respective co-variance matrices:

$$\begin{bmatrix} 1 & 0 \\ 0 & 1 \end{bmatrix}, \begin{bmatrix} 1 & 0.5 \\ 0.5 & 1 \end{bmatrix} \textit{and} \begin{bmatrix} 1 & 0.8 \\ 0.8 & 1 \end{bmatrix}$$

As the off-diagonal elements of the co-variance matrices are increased, the density becomes more compressed towards the 45°line. The extracted contour plots diagrams (Figure 5.23), for the same before mentioned examples give a better

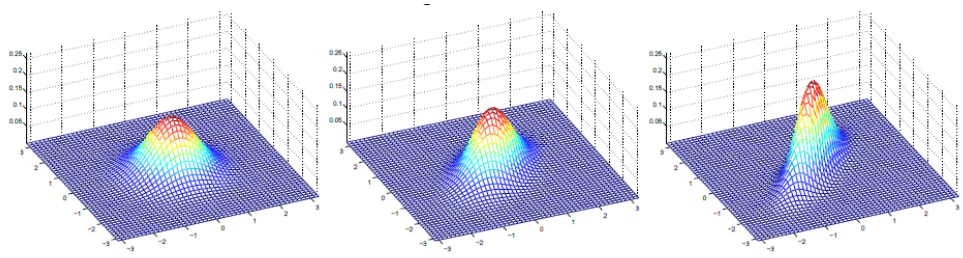

Figure 5.22: Different examples of Gaussian distributions with various co-variance matrices (Ng [2000])

representation of the conclusions as the elimination of the elevation gives a clear image of the slopes and deviations of distributions.

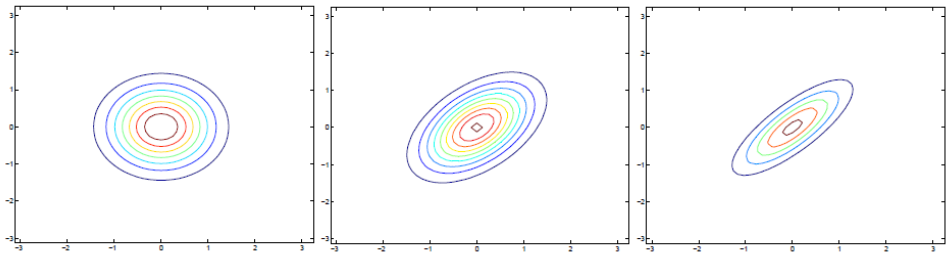

Figure 5.23: Contour plots from the before mentioned Gaussian distributions(Ng [2000])

The matching scores of the response images are extracted and elevation graphs give a clear representation of the distribution of the values as it is shown in Figures 5.24 and 5.25. Either linear or only peak areas have the highest values resulting to representations similar to the ideal cases that above mentioned. It is important to mention that insights that are drawn from the response image, give also significant information about the input images. For instance, if there is a clear linear bright part in the response, linear elements are matched in the input images as building structures, or the ground level.

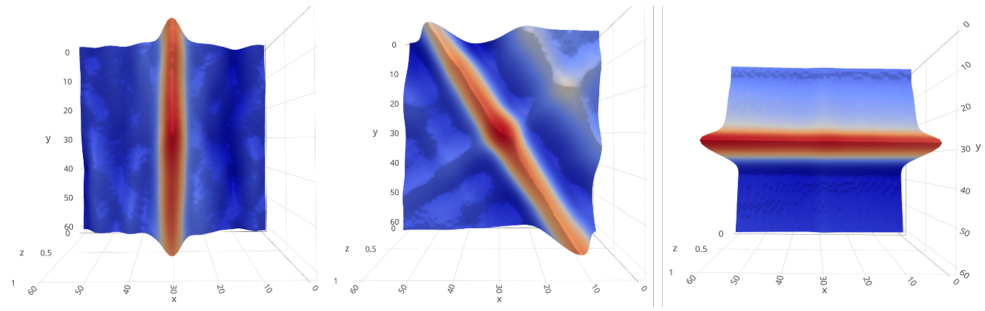

Figure 5.24: Response images having the higher values in a linear arrangement

5.4.7 Correlation between axes

The association between two sets of variables x and y is also of great interest in this case. X and y are considered to be associated if the values of one variable

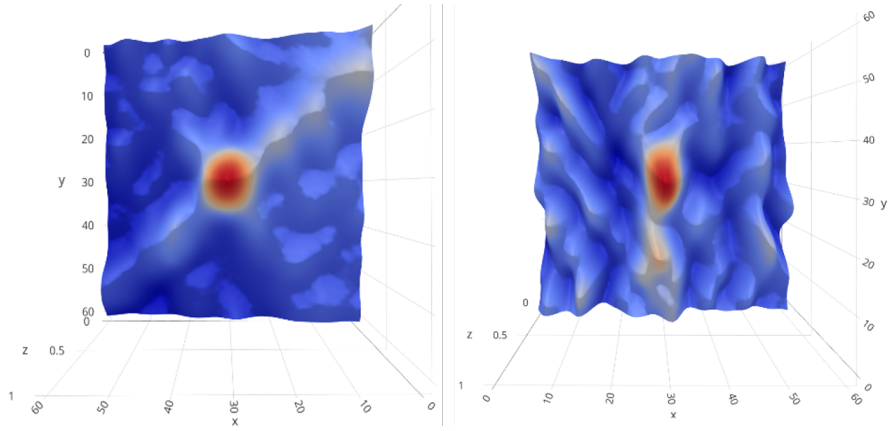

Figure 5.25: Response images having the higher values only in the central part of the image, in a specific peak

affect also the values of the other. On the other hand, x and y values are said to be independent when changes in one variable do not affect the other. Typically, the correlation coefficient reflects the association between the variables.

Consequently, a positive correlation exists when the increase in x values leads to increase in y values. Negative correlation occurs when an increase in x values, gives a decrease in y values or the vice versa. Many types of correlation can describe the association between the values. Pearson's correlation coefficient (ρ) is a commonly used measure for normally distributed data. It is defined as the ration of the co-variance between two variables to the product of their respective standard deviations (Chok [2010]):

$$\rho = \frac{Covariancematrix(x,y)}{\sigma_x \sigma_y}$$

Also the correlation is an important parameter as it is used for the orientation of the ellipses. The angle of the ellipsis in the contour plots is defined by an equation that uses standard deviations in two dimensions and their correlation:

$$angle = \frac{1}{2} atan \frac{\rho \sigma_x \sigma_y}{\sigma_x^2 - \sigma_y^2}$$

5.4.8 Outcome of estimating the correlation between the axes of the response images

Correlation between the axes of the response images gives insights about how transformations for both axes are connected. If a correlation exists, either positive or negative, it is implied that the perfect matching of the input images is achieved when transformations are applied in both axes of the image at the same time. In different case, where correlation is zero, even if transformations are applied to both axes simultaneously, the perfect matching will not be achieved because there is no

association between the axes. Examples with different correlations between two dimensions of a response image are presented in Figures 5.26 and 5.27. The first example shows a result in which correlation has a small number of 0.5 while the second example presents a response image with correlation between the axes equals to 0.98.

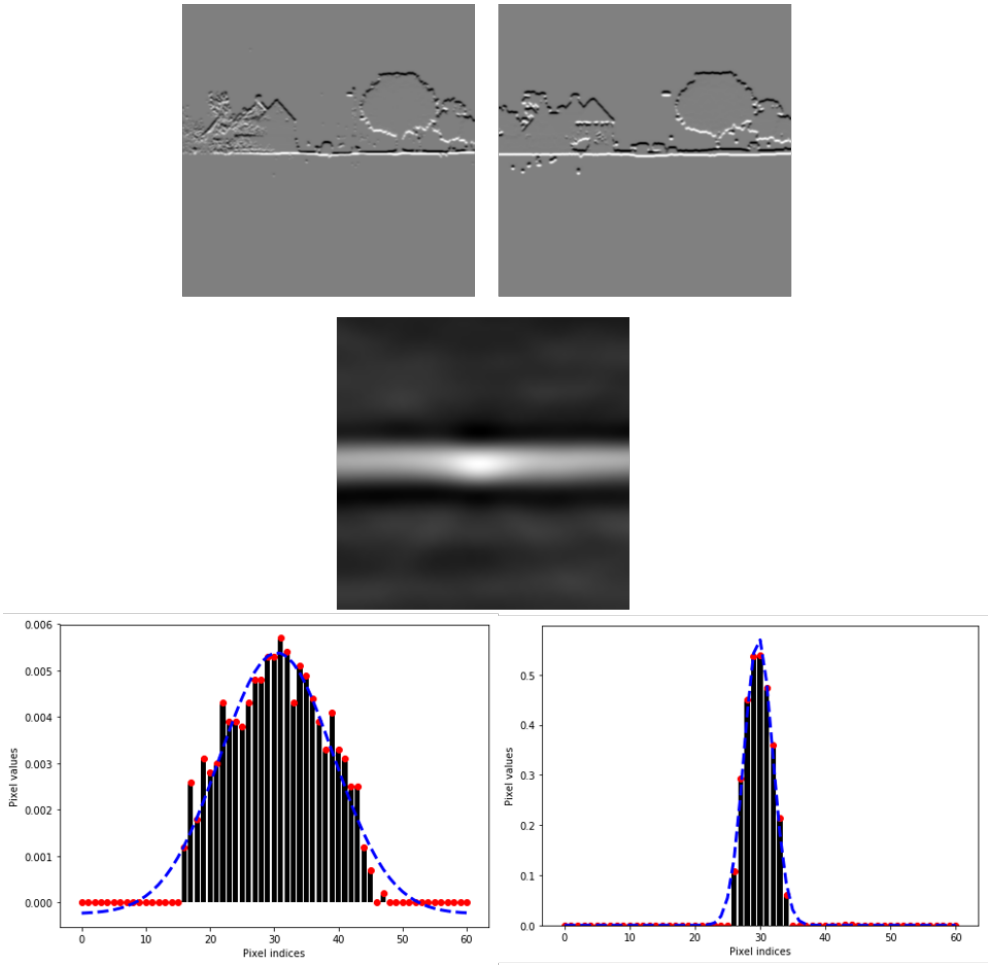

Figure 5.26: At the top the input images, in the middle the response image and at the bottom the distribution of values per row and column in a example where the correlation between the axes has a small value of 0.5

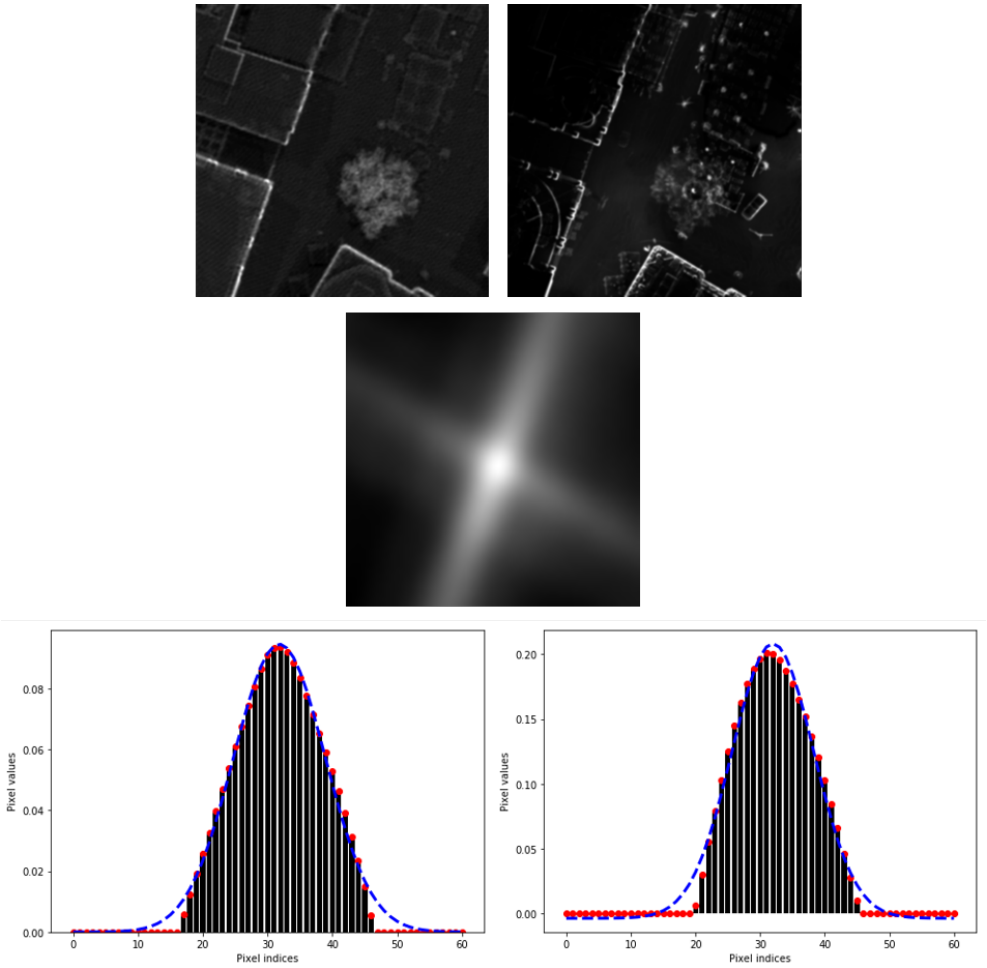

Figure 5.27: At the top the input images, in the middle the response image and at the bottom the distribution of values per row and column in a example where the correlation between the axes has a big value of 0.98

Different values in correlations create different ellipses with different axes and orientations. The first example (Figure 5.26) which depicts a small correlation between axes leads to an ellipse with a big semi-major axis, while the second example (Figure 5.27) leads to an ellipse with smaller axes and quite similar between them, as it can be seen in Figure 5.28. Ellipses that resemble circles indicate a smaller standard deviation and a higher correlation between the measurements and vice versa.

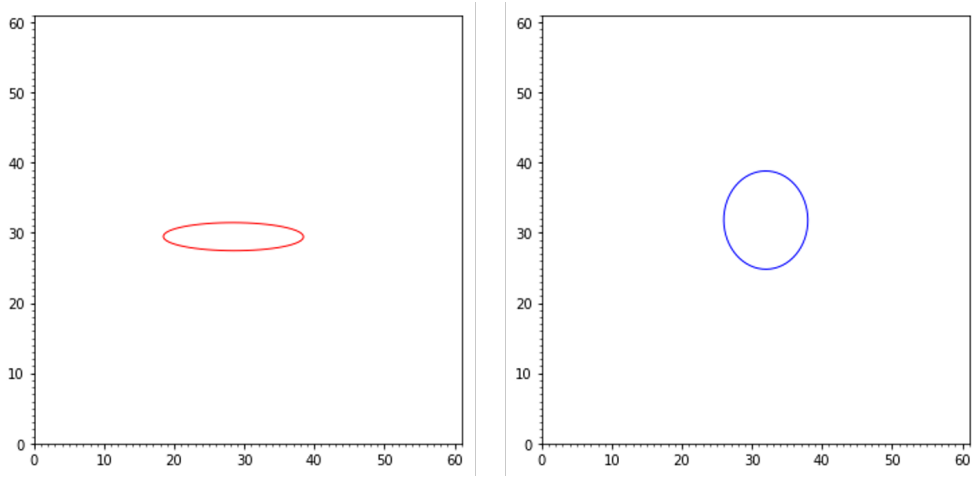

Figure 5.28: Different examples of calculated ellipses from different response images. The first ellipse is calculated from response image depicted in Figure 5.26 and indicates a small correlation, as the semi-major axis is significant bigger than the semi minor axis, while the second ellipse is the respective one for Figure 5.27 and indicates a high correlation as it has similar semi major and semi minor axes and it reminds a circle.

5.4.9 Calculation of the shift

The ultimate target of this work is to quantify the quality of each image and use an indicator that characterizes it. So, each response image for every attribute type is being evaluated and a weight will be assigned to it. The weights are based on the standard deviations and the shift parameters in two axes of each tile. The shift is the parameter that gives an insight about where is located the best matching between the input images or with other words where is the peak value of the response image.

For response images that satisfy both normality tests for values per row and column, and after fitting a line to the individual values the shift parameter is calculated. Using the fitted line, the peak of the line is slightly different from the peak of the bar plot that is the maximum value of the pixels. A more accurate result is again achieved by using the line instead of the individual pixel values.

The matching with zero shift is the one that is achieved when the centers of the input images perfectly coincide. In different case, the shift parameter is equal to the distance between the center of the response image an the location of the peak of the pixel values. As peak it is considered the highest value of the fitted line and not the highest value among the pixel values of the image. A typical calculation of the shift parameter per row and column of the response image of the density attribute (5.29), the shift is calculated from the distance between the location of the center (red line) and the peak value of the fitted line (blue line). Figure 5.30 presents the calculations per row and column respectively.

The length, direction and thickness of each arrow indicate important parameters. The calculated shifts in two dimensions are treated as vectors. The length of the arrow is calculated from the magnitude of the vectors in two dimensions (sum in 5.31) and depicts the value of the shift for the respective response image. The slope of the arrow gives the direction of the shift and it is calculated from the

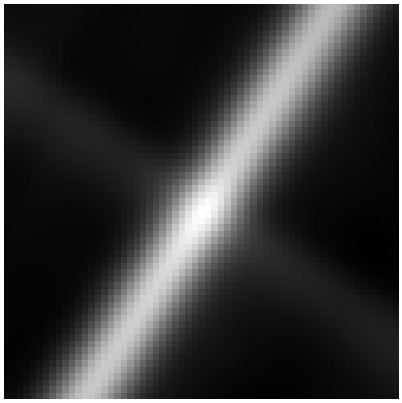

Figure 5.29: Response image

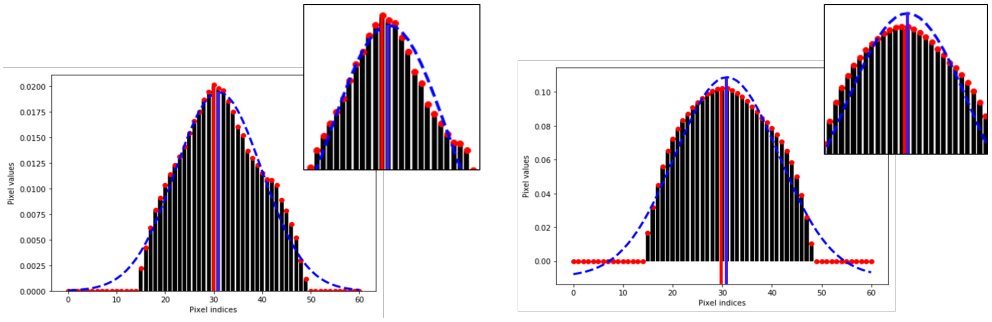

Figure 5.30: Calculation of the shift parameter per row and column. The red line indicates the location of the highest value of the individual pixel values. The blue line indicates the highest value of the fitted line.

trigonometric functions of the vectors (angle θ). Lastly, the thickness of the arrow occurs from the combination of standard deviations in two axes (Figure 5.31). A small standard deviation creates a thicker arrow while a bigger value leads to a thinner arrow.

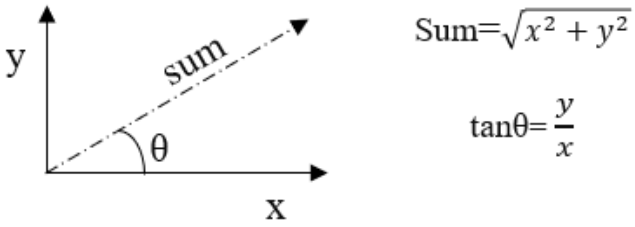

Figure 5.31: Vectors are used for representing the resulting shifts for each response image. The sum refers to the length of the shift and angle θ to its direction.

5.4.10 Outcome of calculating the shift parameter

The shift parameter is calculated for every result of a local co-registration and a value is assigned to the respective arrow in the respective tile. The shift parame-

ters are applied to the center of each tile as they denote the necessary movement. After estimating the shift parameter, it is determined home many pixels the center of the tile has to be shifted and in which direction in order to achieve the best matching.

Another important remark that can be mentioned is that by calculating the shift parameters it is possible to estimate the importance of the tile. By the term importance it is implied, how much the result of a local registration contributes to the global registration based on its quality. When multiple tiles are taken into consideration, in a global registration, shift parameters can be important indicators as if the calculated values are bigger than a specified threshold, or there is not a similar behavior with the adjacent tiles, the tile is considered untrustworthy. In this latter case the assigned weight for the tile is either quite small or zero and the result from the local co-registration does not participate in the global registration.

5.5 RESULTS FOR THE CASE STUDY OF EINDHOVEN

For the ease of the representation, two regions are selected for the analysis using response images extracted from the attribute type of density. Both regions consist of 16 neighboring tiles. The first region is located in the center of the city of Eindhoven and the second one is referring to a region next to the Eindhoven stadium. Both are presented in Figure 5.32.

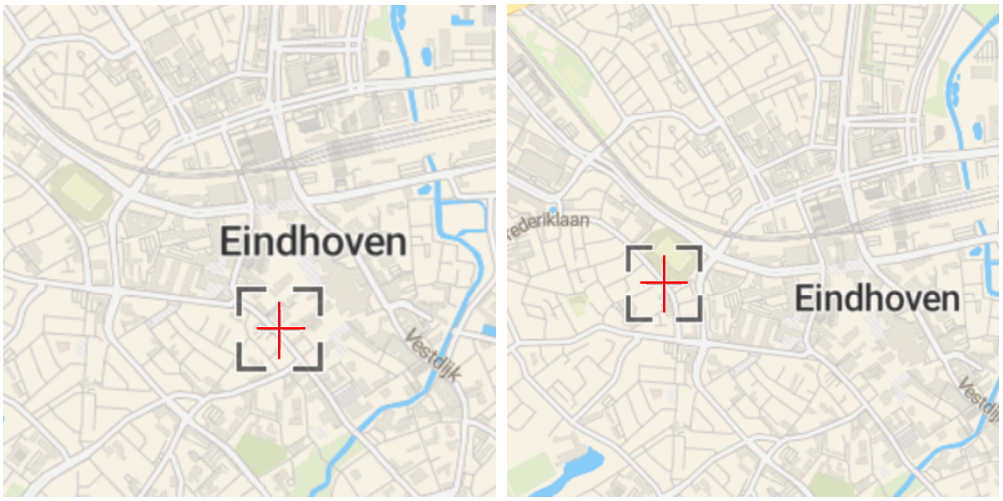

(a) Selected area for analysis in the city center of Eindhoven

(b) Selected area for analysis next to the stadium in Eindhoven

Figure 5.32: Analyzed regions in the city of Eindhoven

Having calculated the standard deviation and the shift parameters for every response image, the next step is to combine all the results of the local pairwise co-registrations into a common frame in order to create a global registration.

Each tile represents a region and it includes information that corresponds to the result of co-registration. Each tile according to the estimated parameters that characterize it, contributes to the global registration with a specific weight. Arrows are used for the visualization of the calculated parameters. Figures 5.33 and 5.34

present the results for the selected regions. Arrows with different lengths, directions and thicknesses have occurred. Longer arrows define bigger shifts and thicker lines indicate smaller standard deviations among the values in the response images.

The first step presents the calculated arrows while the second image characterize the arrows based on their behavior. It is important to be mentioned that the classification of the arrows is very coarse as the classification of the results is based only on one criterion. Red arrows are the ones that deviate from their neighboring tiles only with regard to their direction. Consequently, different weight are assigned to tiles with different information. Empty tiles do not contribute to the global registration as the respective response images did not pass the evaluation criteria. Tiles with red arrows contribute with a small weight as they include faulty measurements and inaccuracies while tiles with white arrows are the reliable results. The weight depends on the length and thickness of the arrows. The shorter and thicker arrows are the best results as they symbolize smaller shifts and standard deviations.

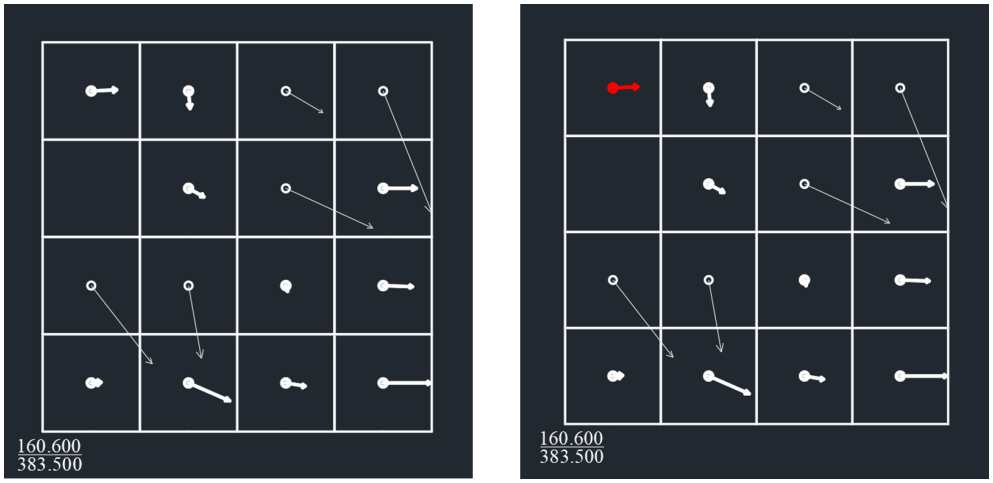

Figure 5.33: The first image presents the calculated arrows for the tiles located next to the stadium of Eindhoven. The second image presents the less reliable result among the tiles, colored red.

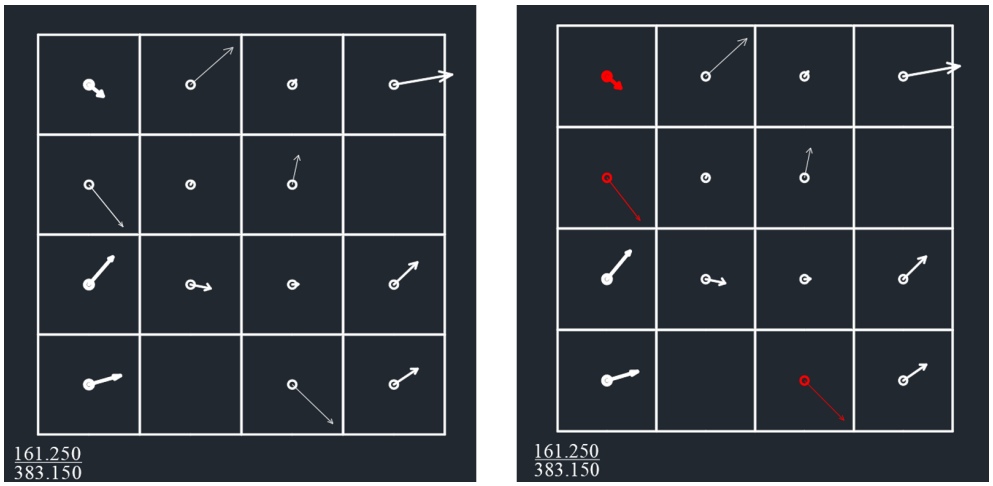

Figure 5.34: The first image presents the calculated arrows for the tiles located in the city center of Eindhoven. The second image presents the less reliable results among the tiles, colored red.

Figures 5.35 shows the respective input and response images for the red arrow existing in Figure 5.34 referring to the city center area while Figure 5.36 explains the red arrow at the bottom of Figure 5.33. Red arrows occur due to errors in datasets as it happens in Figure 5.35 or due to limited similar information in input images as in Figure 5.36.

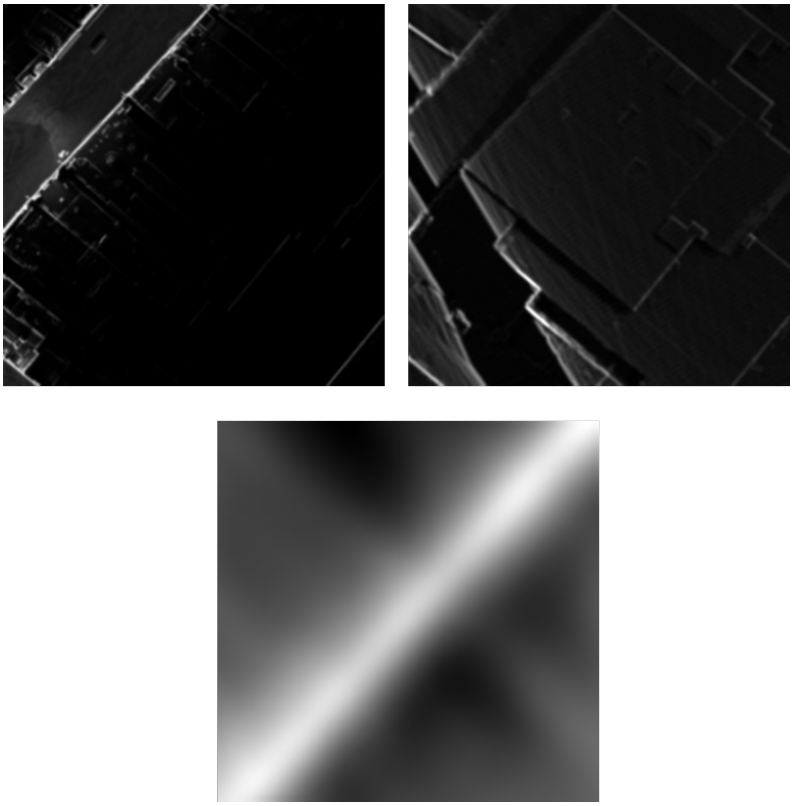

Figure 5.35: At the top the input images and at the bottom the response images for a region that an error in the dataset creates a less good result. This example explains the red arrow in Figure 5.34.

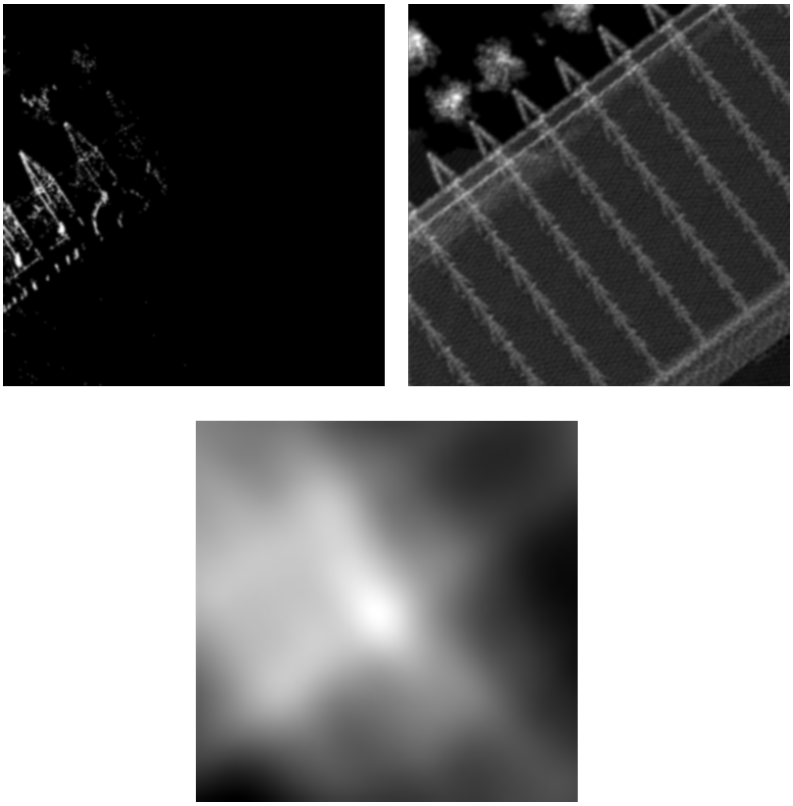

Figure 5.36: At the top the input images and at the bottom the response images for a region that limited common information in the datasets creates a less good result and a blurry response image. This example explains the red arrow at the bottom of Figure 5.33.

The proposed method of characterizing the resulting arrows whether are reliable or not is presented using a binary decision and based only on their direction. This is just an example and a proposal. Further investigation and combined criteria are necessary for a reliable global registration. It is out of scope of this work to simulate the results for neighboring tiles and classify them.

5.6 DISCUSSION

Having calculated the shift parameters for each local pairwise registration may be also beneficial in order to compare the results from the registrations to the trajectory of an MLS platform. Every time, the trajectory of the moving platform is calculated by an integration of vehicle's velocities derived by GNSS processing in combination to an IMU system. However, blocking of the GNSS signal or multi path reflections can decrease the accuracy of the calculations as it is visible in Figure 5.37 where the vehicle is not always possible to acquire signals from at least 4 satellites so to determine its position.

The proper estimation of a vehicle trajectory is estimated using a least squares adjustment method and testing the values of standard deviations among the velocities. High values in standard deviation are translated into a less accurate trajectory calculation.

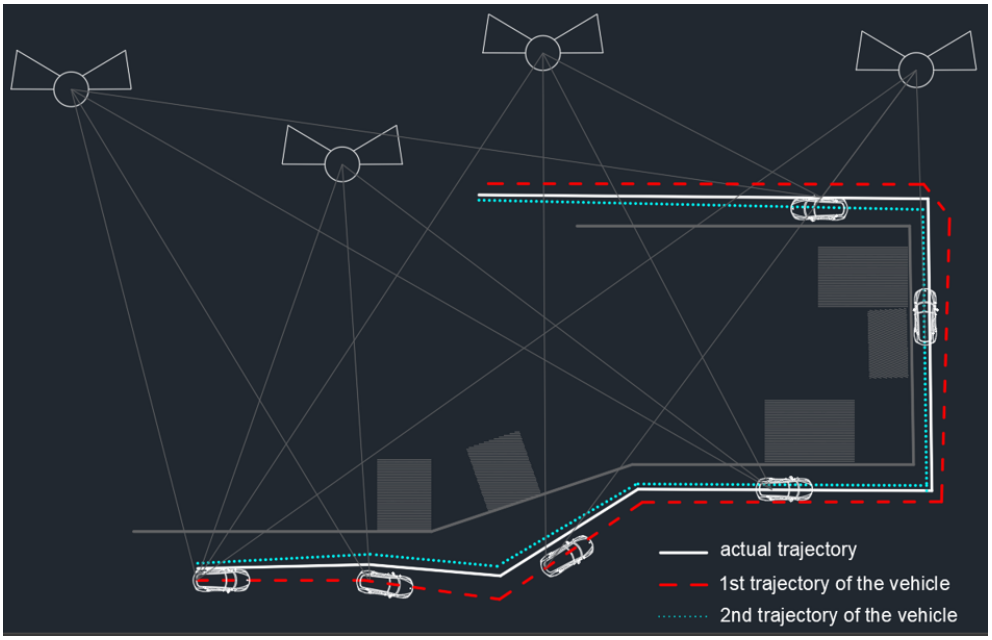

Figure 5.37: The white line presents the actual trajectory of an MLS platform while the red and light blue lines present different trajectories acquired in different times.

Consequently, a shift is also calculated between different calculated trajectories of the vehicle acquired in different times. Every time, the applied shift is assigned according to which trajectory is more accurate in terms of the standard deviation. The trajectory with the smaller standard deviation contributes to the calculation of the final one with a bigger weight while the trajectory with the bigger standard deviation with a smaller weight. Therefore, the adjustment is performed always in the best way with the ultimate target of estimating the trajectory closer to the actual one.

5.7 ROBUSTNESS OF THE METHOD

The term robustness refers to the strength of a method, test or procedure of a work to achieve a good result according to some specific conditions. It also refers to the ability of tolerating perturbations that affect the model's functionality. Recently, robustness tests are becoming integral parts of researches and there is a trade-off between robustness and the degree of adaptability.

As the developed method of this graduation thesis is performed in images, it can be considered a generic approach as the used images can be acquired from co-registrations either from MLS, ALS or TLS data or from different attributes with different characteristics.

As there is not a vast literature of work in the field of the quality of co-registration and in particular for cases for a global registration, robustness of the method can be also connected to the selected size of the tiles for the co-registration. It is commonly believed that smaller tiles will bring higher quality as it is considered that testing in small areas will result to more accurate outcomes.

Also, the usage of smaller tiles helps the reduction of errors as smaller tiles can present uniform characteristics and so less distortions. In cases of urban regions where tiles can be affected by limitations of the system and gross errors do exist, a small tile is useful as the error will be limited only to a small number of values consisting this specific tile and will not affect the quality of neighboring values that may have a better quality. Smaller tiles can also be beneficial as the final result will be less sensitive to local occlusions and limitations. Another advantage of tiles with smaller dimensions is the significant less time during computational performance as iterative processes over big tiles are time-consuming and require appropriate equipment. Lastly, a small tile is considered to be easily manageable but a basic requirement is that at the same time the size of a tile must be significant reliable. It must be as small as to include all the adequate information that characterizes the region and can be compared with another tile and as big as it decreases the possibilities of existing errors and inaccuracies.

5.8 SUMMARY

The whole chapter describes the whole procedure for analyzing the response images acquired from a co-registration of point clouds. The main steps of the implemented method as well as the extracted conclusions are briefly presented below:

- Pixel values are normalized in order to centralize the values and make them more easily comparable while the characteristics of the distributions as mean value and standard deviation remain the same.
- Response images are tested about the distribution of their pixel values for both dimensions of the images.
- Interpolation between discrete pixel values is implemented by fitting a Gaussian model while at the same time a sub pixel accuracy is achieved as the peak of the line is not always the same with the highest matching score that exist in the response images.
- Calculation of standard deviation of images' values is also calculated with sub pixel accuracy as it is computed also by the fitted line.
- Calculation of the amount of pixels that the center of the image must be shifted in order to gain the perfect matching with the co-registration is computed and it can be proved an essential conclusion, useful for a next evaluation of the whole method in a large scale project.
- Correlation between the axes of the response images is another parameter that is estimated, giving insights about the relation between the transformation parameters of the different axes.
- Representative results from selected tiles in two different regions in Eindhoven are presented. Neighboring tiles are combined in order to jump from local pairwise registrations to the global registration.

All the steps are used in order to be able to quantify the quality of the result of a co-registration in terms of precision and reliability with the aim of creating a valuable result. Moreover, the stochastic part of a co-registration that is as important as the functional part is addressed because it needs to be added for a better understanding of the result. The quality of a result is considered as important as the result itself. Results that are accompanied by quality indicators are meaningful and useful for further use. Lastly, by having quality indicators in each result, it is becoming clear which result are more significant and which are less while it is becoming easy to locate the faulty results and possibly estimate the reason of the occurrence.

Lastly, the implemented method analyzes the results from a co-registration using statistical measures and not only visual methods. The main conclusion is that the quality of a matching and hence the degree of the template matching quality, is highly correlated with the distributions of pixel values in response images. The analysis showed that results with a good fit occurred from response images with normally distributed pixel values, while poorer fit occurred from response images that have a more irregular, non normal distribution in their values.

6 CONCLUSIONS AND FUTURE WORK

This chapter includes the extracted conclusions and some recommendations that can be proposed for a future analysis as they occurred during this research. The conclusions will be presented by answering the sub-questions as well as the basic research question that were framed in the beginning.

6.1 RESEARCH QUESTIONS

Some sub-questions that are relevant and set a basis for successfully answer the main research question are :

- **What are the requirements for a registration?**

In order to achieve a successful registration between point clouds acquired from different sources it is important to satisfy some criteria.

· Point clouds and hence input images must include corresponding objects, in order to be possible to calculate similarity scores and therefore representative response images. In examples of input images that do not include similar information, objects are not clear and there are not distinct elements, response images are blurry and distributions of values are not indicative. They are examples of response images with multiple high values, not distinctive peaks or multiple peaks. Such results cannot be used for further analysis and cannot give indications about the quality of the matching. A typical example can be seen in Figure 6.1. The input images are also shown with a transparent background and also colored with different colors in order to be clear the limited similarities exist between them, fact that leads to a blurry response images, a typical example of poor fit, that does not pass the normality test and hence it is not used for analysis. Comparing the response images also with the point clouds that are extracted from, it is clear that limited common information exist in them. Figure 6.2 presents both ALS and MLS point clouds with densities 73,055 and 106,201 respectively.

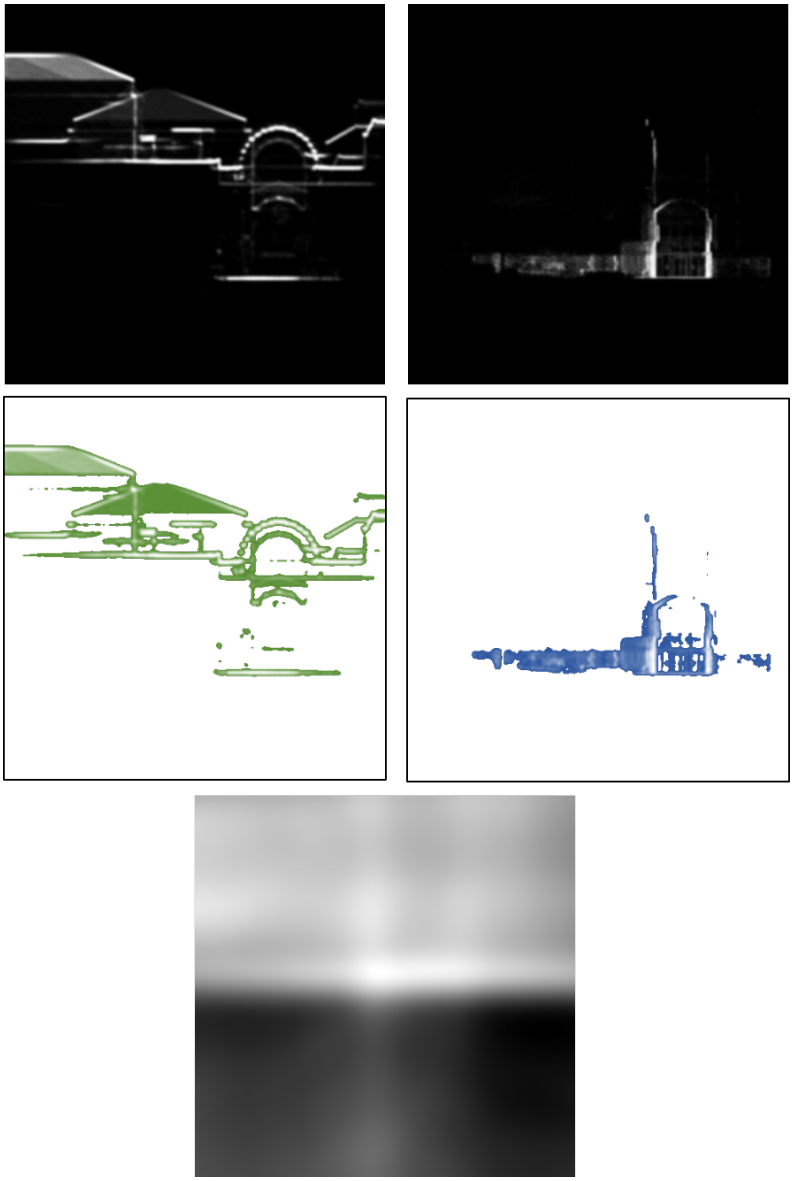

Figure 6.1: Input images with limited similar information create a response image with not discrete bright parts

Figure 6.2: ALS and MLS point clouds depicting the same scene as in Figure 6.1

· Another important requirement for achieving a good registration is the optimal selection of the size tile. A big tile can include errors that cannot be

located while a small tile may not be satisfactory due to limited information. Although it is considered a significant parameter for a successful registration it is not encompassed in the research part of this work and thus the conclusions are taken from a theoretical research.

- **Is this quality assessment technique suitable for every case of co-registration?**

Image-based methods for co-registration can give reliable results and the response images give clear insights, with the prerequisite that images extracted from point clouds are referring to the same area and include similar information. Moreover, using the different attributes of images, better results can be obtained for regions with different characteristics, as for instance by using the density attribute for an environment with building structures but the color attribute for a rural environment with much more vegetation.

Considering that the acquired MLS and ALS data are reliable and accurate, the implemented quality assessment technique can be considered suitable for every case of an image-based method as it quantifies the quality of a procedure taking as input an image. Moreover, it can be also considered a generic approach as it can be used for images extracted using other techniques or from point clouds generated from different devices.

- **How can the probabilistic analysis be performed?**

A probabilistic analysis is performed in order to estimate the quality of the result of a co registration. The evaluation of the result is approached by performing multiple steps:

· The first step includes the computations in order to normalize the response images' pixel values. By calculating the mean values of each row and each column for both dimensions, a new array is created which is further used. By subtracting the general mean of the new array, a normalization of the pixel values is accomplished. Normalization is a necessary step, as it creates homogeneous values, easy to be handled while the distribution characteristics as standard deviations remains unchanged.

· The second step is about interpolating the values. A Gaussian curve is fitted to the individual pixel values, and new intermediate values are generated, giving a more accurate calculation of standard deviation.

· The third step is about calculating the shift parameter for every response image. By using the fitted line, the peak value is the one occurred from the line and not the highest value among the pixels. The shift parameter is calculated by comparing the location of the peak value and the center of the image. A positive or negative shift parameter gives indications about the direction of the required movement of the center of the image.

· Lastly, a weight is assigned to each response image by comparing the calculated shift parameter and the standard deviations in both dimensions. Arrows are used to represent the weights. Different lengths and slopes indicate the size and direction of the shifts while thickness is characterized by standard

deviations.

- **Could a probabilistic analysis reveal that the requirements are not met?**

A probabilistic analysis is actually a way to justify if the requirements for a registration are met or not. By analyzing the results a clear insight about them is provided. Analyzing only the visual part of the response images do not always give the proper knowledge. A deeper analysis using statistical terms has proved to be valuable as multiple errors are detected even in cases where the visual result was quite satisfying. Moreover, the main advantage of this work is that the results are judged and therefore classified based on an analysis of their distributions and not on randomly specified thresholds. It is not a procedure to find the best number as a threshold but a whole analysis that characterizes the results.

Generally, quality in terms of precision and reliability, gives in each result an extra value as it characterizes the degree of satisfying predefined demands. For instance, in a co-registration that a high precision is important, only results that have small standard deviations are used. Figure 6.3 presents the main consecutive steps of this research and the conclusions that can be derived for each case.

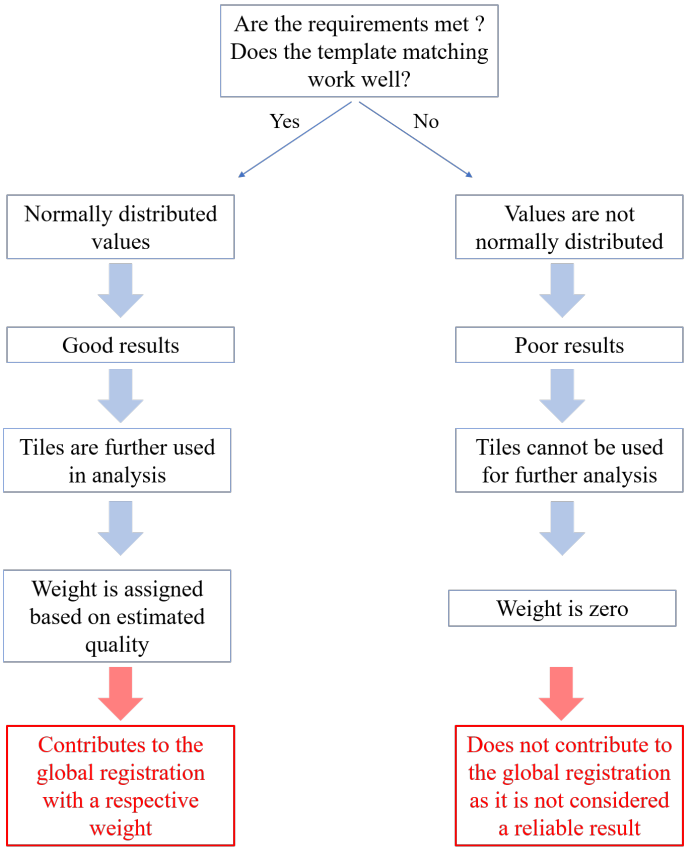

Figure 6.3: A schematic representation that indicates the workflow of the implemented method

After answering the sub-questions, the main research question can be answered.

- **To what extent is it possible to estimate the probabilistic aspects of the result of a co-registration between aerial and mobile laser scanned point clouds ?**

There are various ways to co-register points clouds and different results that can be obtained. As this work focused on an image based registration method, the results that are used and analyzed are response images. The response images and therefore the pixel values of the images are pre-processed and tested for their distribution. After implementing the normality tests, only response images that have normally distributed pixel values are tested. Two indicators are analyzed, the reliability and the precision constituting the probabilistic aspects of the result of a co-registration.

Reliability is theoretically defined as the probability of success. It is also defined as the degree of detecting errors in the datasets and how much do affect the final estimations. Reliability is examined using both internal and external reliability.

Internal reliability

In order to judge the internal reliability of the final estimations, it is checked in which degree the errors are detected. In this specific work, an error is a faulty registration with an undesirable matching. A proper registration gives a response image with clear discrete brighter parts either linear or only peak areas. On the contrary, faulty registrations do not give response images with clearly detectable brighter parts, but fuzzy and blurry images. The visual part of the response image is highly correlated to the distribution of the pixel values and therefore the quality of the matching. As a result, to determine the internal reliability and how well the errors of the implemented method are detected, the number of response images that passed the normality tests and they do not include significant errors or deviations is compared to those having different distributions, outliers or multiple peaks.

External reliability

The term external reliability assess the consequences of the result, when errors and disturbances remain undetected. It describes the influence of these errors to the data. Results from co-registration containing errors have poor external reliability and hence an equivalent weight is assigned to them. Response images that have errors that are not detected through the analysis may occur due to the selected significance level of the statistical tests. When a significance level is selected, a corresponding confidence level that determines the range of likely values is also set. That means that by setting a significance level, there is a probability that a number of results do not satisfy the statistical tests and hence they are potential erroneous response images.

In this research, the significance level is set to 0.005 and that it is translated to a 0.5 % of probability to have response images that do not pass the criteria and present some error. The errors can be multiple existing peaks, especially small ones that are not taken into consideration as they are not detected by the selected method. By fitting a line to the discrete pixel values, small peak regions, especially at the tails of the distribution are not considered significant and are neglected. Typical examples

with multiple peak areas are shown in Figure 6.4.

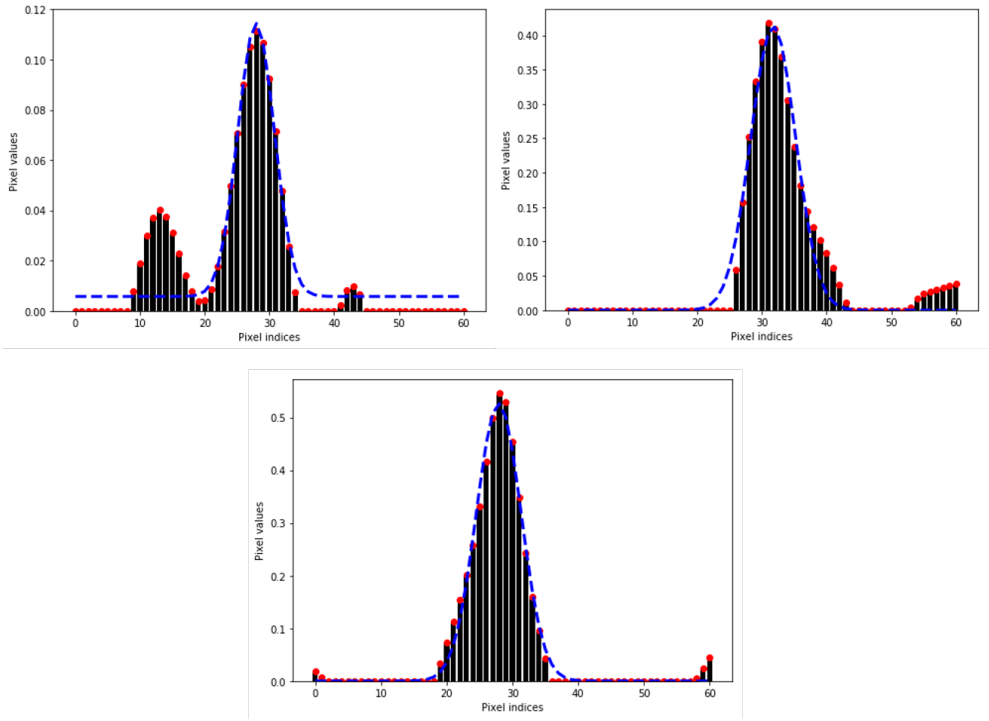

Figure 6.4: Response images containing having more than one significant peak areas either at the central part or at the tais

Precision

In order to analyze the precision of the result of a co-registration, the standard deviation of the pixel values of the response images in both axes is calculated. The standard deviation characterizes the precision and it can be correlated to the existence of errors. The smaller the standard deviation, the smaller the disparity and the variability among the values and the better the precision of the result. Since the pixel size of the images is 10 cm, a result is precise when the standard deviation is smaller than that number. Considering also that a sub-pixel accuracy is achieved, a highly precise result must have an even smaller standard deviation.

Classifying the results based on the values of standard deviation is not considered useful as it would entail a degree of randomness as random classes and random thresholds would be applied. On the other hand, in case of a large scale project, with many tiles, it would be beneficial to compare the calculated values of standard deviations between the neighboring results and find a way to determine whether or not they fit to the neighbor's behavior. So, it is becoming clear that estimating how precise is the result itself is not only related to the actual value but a correlation with all the calculated values in a specific defined area.

6.2 SIGNIFICANCE OF THIS RESEARCH

With this graduation thesis an estimation of the quality of the results of a co-registration between point clouds is introduced. The method includes an analysis of the response images and it is considered generic as it can be applied with limited modifications for every image. It is not a trivial task to determine the quality of an alignment of matched point clouds but this is a method that brings a probabilistic analysis of a result. Quality indicators are provided based on the precision and reliability of the data used. Usually in the majority of the previous works the quality of the matching was tested by comparing the result with the ground truth situation due to the small size of datasets. The current approach of evaluating a result of co-registrations can be applied also to large scale projects including spatial information for a city or a whole country. In such cases, due to the vast amount of data, it is not doable to judge each individual result visually one by one or compare with the ground truth and therefore it is necessary to use automated processes.

By applying the implemented method in results of co-registrations, a procedure similar to error propagation is performed. As the errors are distributed based on certain criteria, weights are assigned to each result based on its calculated quality indicators. It is therefore a way to create a global registration by combining all the local registrations according to their significance but also locate the largest residuals within the dataset.

Generally, the correctness and quality of the data is crucial. Especially in the field of the spatial information and when dealing with the real world, it is important to estimate the quality of the result as faulty conclusion can cost time and money spent. Not knowing the quality of the match, may lead to erroneous manipulations.

As 3D point clouds constitute an important source of spatial information in many fields, a measure for quantifying the quality of the integration of different datasets is beneficial and can be applied in multiple fields of expertise as for example in 3D urban modeling, indoor modeling, flood modeling, automated driving or deformation survey for construction of roads, tunnels, bridges, damns. 3D point clouds acquired from ALS techniques can also be used for forest mapping or characterizing the distribution of vegetation for accurate estimations of its area, biomass or volume. The diverse use of the 3D spatial information forces to focus not only to the acquisition and integration of information but also to evaluate the quality of the outcomes for avoidance of inaccuracies.

6.3 FUTURE WORK

This section presents a few recommendations that can be helpful and valuable in a potential expansion of this work. They are remarks that occurred during the analysis and implementation and can be addressed in future works. Approaching the stochastic parts of a model and characterizing the quality of a co-registration

is an ambitious and challenging topic and it should be always in the center of interest.

- This approach used the result of an image based co-registration between MLS and ALS point clouds taking into consideration the translational errors that occurred during the integration of datasets. Further analysis can be done including also potential rotation or scale errors that may exist in datasets.
- The probabilistic aspects analyzed only for the result of a local registration. Only the response images contributed to the estimation of the quality. It should be beneficial to characterize the precision and the quality of each dataset individually. In other words, except from quantifying the quality of the integration part, it is significant to evaluate also the datasets after the acquisition part. Knowing the quality of point clouds acquired from different sources may enhance also the quality of the integration part as the transformation parameters will be applied to the less good dataset. For instance, in cases of urban environments, MLS techniques may generate less good point clouds compared to ALS, due to positioning errors or reflections from objects existing in the scene. In that cases, the transformation parameters should be applied to MLS datasets. On the contrary, in rural environments it may be beneficial to apply the transformation parameters to ALS datasets.
- This work presents a method for quantifying the quality of a single response image. It would add an extra value to the result if multiple response images acquired from different attribute types but referring to the same area, create an aggregate response image based on the quality of each attribute type.
- A suggestion about having a more reliable global registration would be to define a model that simulates the behavior of all the arrows in the tiles and characterizes whether they are reliable or not based on their deviation in length, direction, thickness or ideally in an combination of all three. A possible way to examine the resulting arrows in consecutive and neighboring tiles could be by testing the degree of fitting into a spline.
- Moreover, this work used response images extracted from projections of 3D point clouds to 2D images. A more accurate result could be acquired if 3D template matching was performed using at the same time transformations in all 3 directions with the prerequisite that the procedure will be doable in respect to time and memory needs.
- Another suggestion could be to test the distribution of images' values using formulas for 2D instead of testing values per row and values per column separately by implementing tests in 1D. A 2D analysis may result to a better calculation of the ellipses as their axes will correspond to the eigen-vectors of the covariance matrix and it may lead to a better fit to the images' pixel values.
- Another suggestion could be to test different distributions and the degree of their fitting to the pixel values. In that work, values are tested only whether or not they satisfy a test for normal distribution. A further analysis using also other distributions may reveal that the fitting of the line to the pixel values is

better, the distances between the pixel values and the line is minimized and the sub-pixel accuracy is more efficient.

Finally, this work sets an important basis for estimating the quality of a result of a co-registration by quantifying the existed errors. It can be expanded based on the recommendations, enriched and be used in every image based registration when it is necessary to combine multiple local pairwise registration in a global frame.

BIBLIOGRAPHY

Baarda, W. (1968). A testing procedure for use in geodetic networks. *Netherlands geodetic commission*, 2(5).

Bae, K.-H. and Lichti, D. D. (2008). A method for automated registration of unorganised point clouds. *ISPRS Journal of Photogrammetry and Remote Sensing*, 63(1):36–54.

Bellekens, B., Spruyt, V., Berkvens, R., Penne, R., and Weyn, M. (2015). A benchmark survey of rigid 3D point cloud registration algorithm. *International Journal on Advances in Intelligent Systems*, 8(1):118–127.

Benjemaa, R. and Schmitt, F. (1999). Fast global registration of 3D sampled surfaces using a multi-z-buffer technique1. *Image and Vision Computing*, 17(2):113–123.

Bergevin, R., Soucy, M., Gagnon, H., and Laurendeau, D. (1996). Towards a general multi-view registration technique. *IEEE Transactions on Pattern Analysis and Machine Intelligence*, 18(5):540–547.

Besl, P. J. and McKay, N. D. (1992). A method for registration of 3D shapes. *IEEE Transactions on Pattern Analysis and Machine Intelligence*, 2(239–256).

Bogoslavskyi, I. and Stachniss, C. (2017). Analyzing the quality of matched 3D point clouds of objects. In *2017 IEEE/RSJ International Conference on Intelligent Robots and Systems (IROS)*, pages 6685–6690. IEEE.

Boise State University, . (2019). The runge phenomenon. https://math.boisestate.edu/~calhoun/teaching/matlab-tutorials/lab_11/html/lab_11.html, last assessed on April of 2019.

Burghouts, G., Smeulders, A., and Geusebroek, J. (2008). The distribution family of similarity distances. In *Advances in neural information processing systems*, page 201–208.

Chen, Y. and Medioni, G. (1992). Object modelling by registration of multiple range images. *Image and vision computing*, 10(3):145–155.

Chetverikov, D., Svirko, D., Stepanov, D., , and Krsek, P. (2002). The trimmed iterative closest point algorithm. in object recognition supported by user interaction for service robots.

Chok, N. S. (2010). *Pearson's versus Spearman's and Kendall's correlation coefficients for continuous data.* PhD thesis, University of Pittsburgh.

Christodoulou, A. (2018). An image-based method for the pairwise registration of mobile laser scanning point clouds. Master's thesis, TU Delft.

Ding, L., Goshtasby, A., and Satter, M. (2001). Volume image registration by template matching. *Image and Vision Computing*, 19(12):821–832.

Gaidhane, V., Hote, Y., , and Singh, V. (2014). A computationally efficient approach for template matching-based image registration. *journal Sadhana*, 2(317–331).

Gümüş, K., Gümüş, M., and Erkaya, H. (2017). A statistical evaluation of registration. *APPLICATIONS. Mediterranean Archaeology Archaeometry*, 17(3).

Godin, G., Rioux, M. B., and R. (1994). Three-dimensional registration using range and intensity information. In *Proc. SPIE 2350, Videometrics III*.

Guizilini, V. and Ramos, F. (2018). Iterative continuous convolution for 3D template matching and global localization.

Jurie, F. and Dhome, M. (2001). Real time 3D template matching. In *Proceedings of the 2001 IEEE Computer Society Conference on Computer Vision and Pattern Recognition. CVPR 2001*, volume 1, pages I–I.

Kamgar-Parsi, B., Jones, J., and Rosenfeld, A. (1989). Registration of multiple overlapping range images: Scenes without distinctive features. In *Computer Vision and Pattern Recognition, 1989. Proceedings CVPR'89., IEEE Computer Society Conference on*, page 282–290.

Kumar, V. and Gupta, P. (2012). Importance of statistical measures in digital image processing. *International Journal of emerging technology and advanced engineering*, 2(8):56–62.

Kutterer, H., Seitz, F., Alkhatib, H., and Schmidt, M. (2016). *1st International Workshop on the Quality of Geodetic Observation and Monitoring Systems*. Springer.

Le Moigne, J., Cole-Rhodes, A., Eastman, R., El-Ghazawi, T., Johnson, K., Knewpijit, S., Laporte, N., Morisette, J., Netanyahu, N. S., Stone, H. S., et al. (2002). Multiple sensor image registration, image fusion and dimension reduction of earth science imagery. In *Proceedings of the Fifth International Conference on Information Fusion. FUSION 2002.(IEEE Cat. No. 02EX5997)*, volume 2, pages 999–1006. IEEE.

Leica Geosystems, . (2019). Leica citymapper airborne hybrid sensor. https://leica-geosystems.com/products/airborne-systems/leica-citymapper, last assessed on June of 2019.

Lemmens, M. (2011). *Geo-information: technologies, applications and the environment*. Springer Science & Business Media.

Lin, C.-C., Tai, Y.-C., Lee, J.-J., and Chen, Y.-S. (2017). A novel point cloud registration using 2D image features. *EURASIP Journal on Advances in Signal Processing*, 2017(1):5.

Lu, F. and Milios, E. (1997). Globally consistent range scan alignment for environment mapping. *Autonomous robots*, 4(4):333–349.

MIT Open Courseware, . (2019). Kolmogorov-Smirnov test. https://ocw.mit.edu/courses/mathematics/18-443-statistics-for-applications-fall-2006/lecture-notes/lecture14.pdf, last assessed on June of 2019.

Mitra, N., Gelfand, N., Pottmann, H., and Guibas, L. (2004). Registration of point cloud data from a geometric optimization perspective. In *Proceedings of the 2004 Eurographics/ACM SIGGRAPH symposium on Geometry processing*, page 22–31.

Ng, A. (2000). Lecture notes for the course with code CS229, Stanford University. volume 1. https://sgfin.github.io/files/notes/CS229_Lecture_Notes.pdf, last assessed on June of 2019.

Ober, P. B. (2004). Integrity prediction and monitoring of navigation systems.

Ogaja, C. A. (2011). *Applied GPS for Engineers and Project Managers*. American Society of Civil Engineers.

Parmehr, E., Fraser, C., Zhang, C., and Leach, J. (2012). Automatic Registration of Aerial Images with 3D LiDAR Data Using a Hybrid Intensity-Based Method. In *2012 International Conference on Digital Image Computing Techniques and Applications (DICTA)*, page 1–7.

Pulli, K. (1999). Multiview registration for large data sets. In *Second International Conference on 3D Digital Imaging and Modeling (Cat. No. PR00062)*, pages 160–168. IEEE.

Reddy, B. and Chatterji, B. (1996). An fft-based technique for translation, rotation, and scale-invariant image registration. *IEEE transactions on image processing*, 5(8):1266–1271.

Ripperda, N. and Brenner, C. (2005). Marker-free registration of terrestrial laser scans using the normal distribution transform. *Proceedings of the ISPRS working group*, 4.

Sharp, G., Lee, S. W., and D.K. (2002). ICP registration using invariant features. *IEEE Transactions on Pattern Analysis and Machine Intelligence*, 1(90–102).

Shetty, A. (2017). *GPS-LiDAR sensor fusion aided by 3D city models for UAVs*. PhD thesis, University of Illinois at Urbana-Champaign.

Someren, B. v. (2016). Comparing features for point cloud registration with varying densities. Technical report.

Sweco (2019). Move 3 user manual version 4.4.

Teo, T. and Huang, S. (2014). Surface-based registration of airborne and terrestrial mobile lidar point clouds. *Remote Sensing*, 6(12):12686–12707.

Teunissen, P. (1998). Quality control and GPS. In *GPS for Geodesy*, page 271–318. Springer, Berlin, Heidelberg.

Teunissen, P., Simons, D., and Tiberius, C. (2005). Probability and observation theory. In *Probability and Observation Theory*. Faculty of Aerospace Engineering. Technical University of Delft.

Theiler, P. (2015). *Automated Registration of Terrestrial Laser Scanner Point Clouds*. PhD thesis, ETH Zurich.

Trucco, E., Fusiello, A. R., and V. (1999). Robust motion and correspondence of noisy 3D point sets with missing data. *Pattern Recognition Letters*, 9(889–898).

VanCourt, T., Gu, Y., and Herbordt, M. C. (2005). Three-dimensional template correlation: object recognition in 3D voxel data. In *Seventh International Workshop on Computer Architecture for Machine Perception (CAMP'05)*, pages 153–158. IEEE.

Velodyne 32-E High Definition LiDAR Sensor, . (2019). User's manual and programming guide. https://velodynelidar.com/lidar/products/manual/63-9113%20HDL-32E%20manual_Rev%20G.pdf, last assessed on June of 2019.

Wang, J., Lindenbergh, R., Shen, Y., and Menenti, M. (2016). Coarse point cloud registration by EGI matching of voxel clusters. *ISPRS Annals of the Photogrammetry, Remote Sensing and Spatial Information Sciences*, 3:97.

Weinmann, M. and Jutzi, B. (2015). Geometric Point Quality Assessment for the Automated, Markerless and Robust Registration of Unordered TLS Point Clouds. *ISPRS Annals of Photogrammetry, Remote Sensing & Spatial Information Sciences*, 2.

Wikipedia, . (2019). Kolmogorov-Smirnov test. https://en.wikipedia.org/wiki/Kolmogorov%E2%80%93Smirnov_test, last assessed on June of 2019.

Williams, S., Bock, Y., Fang, P., Jamason, P., Nikolaidis, R., Prawirodirdjo, L., and Johnson, D. (2004). Error analysis of continuous GPS position time series. *Journal of Geophysical Research: Solid Earth*, 109(3).

Wolberg, G. and Zokai, S. (2000). Image registration for perspective deformation recovery. In *Automatic Target Recognition X*, volume 4050, pages 259–271. International Society for Optics and Photonics.

Zhang, G., Lei, M., and Liu, X. (2009). Novel template matching method with sub-pixel accuracy based on correlation and fourier-mellin transform. *Optical Engineering*, 48(5):057001.

Zhu, N., Marais, J., Bétaille, D., and Berbineau, M. (2018). GNSS position integrity in urban environments: A review of literature. *IEEE Transactions on Intelligent Transportation Systems*, (99):1–17.

A REFLECTION

Quality is not an act. It is a habit.

Aristotle

This section presents the relationship between the methodical line of approach of the Master Geomatics and the method chosen by the student in this framework.

Studies at TU Delft as well as in the Geomatics Master motivate the students to delve into the subject of their thesis after a detailed literature review. As a result, all the implemented methods are a combination of research but also personal contribution in terms of critical thinking and creativity. Especially, with this graduation thesis, a method to approach the stochastic part of a co registration between point clouds and therefore an evaluation of the quality of the result is implemented. Although this work takes some assumptions about the quality of the acquisition of the datasets it can be considered a work of paramount importance. It is considered that the evaluation of the result is as important as the result itself. Presenting a result, without a quality indicator and a reliable comparison is just a number without an actual value.

Moreover, the conducted research is quite important especially for the wider field of Geomatics including the commercial field. The analyzed method can contribute to more reliable global registrations in the future. Integration of datasets referring to whole cities or countries require the evaluation of a vast amount of data and therefore it is useful to minimize the required time for the evaluation of the results. As this thesis presents an automated way for estimating the quality it can be considered an important contribution.

Overall, my goal throughout this graduation thesis is totally achieved as I delved into the field of point clouds and I conducted a research about a piece of the chain of the co-registration by estimating the quality of the results of co registration of point clouds, field that has limited investigated in the past.

COLOPHON

This document was typeset using LaTeX. The document layout was generated using the arsclassica package by Lorenzo Pantieri, which is an adaption of the original classicthesis package from André Miede. The figures and plots are generated using Matplotlib and Plotly. BibTeX was used to generate the bibliography.